OUKA
Osaka University Knowledge Archive

Title	Studies on a Novel Process for Nitrogen Utilization using Iron-based Intermetallic Compounds
Author(s)	伊東, 正浩
Citation	大阪大学, 2001, 博士論文
Version Type	VoR
URL	https://doi.org/10.11501/3184300
rights	
Note	

Osaka University Knowledge Archive : OUKA

https://ir.library.osaka-u.ac.jp/

Osaka University

Studies on a Novel Process for Nitrogen Utilization using Iron-based Intermetallic Compounds

(鉄系金属間化合物を用いた新規窒素利用プロセスに関する研究)

2001

Masahiro Itoh

Department of Applied Chemistry

Faculty of Engineering

Osaka University

Preface

The work presented in this thesis has been carried out during 1998-2000 under the guidance of Professor Gin-ya Adachi at Department of Applied Chemistry, Faculty of Engineering, Osaka University.

This thesis deals with nitrogen absorption and desorption characteristics for iron-based intermetallic compounds and a novel reaction process using highly reactive atomic nitrogen absorbed in the intermetallic compounds. The results and findings obtained through this work gave important information on the storage technique of nitrogen and high efficient reaction using atomic nitrogen. This fundamental work is expected to contribute to the further development of the nitrogen storage materials and their applications.

Masahiro Itoh

Department of Applied Chemistry

Faculty of Engineering

Osaka University

Yamada-oka,

Suita, Osaka, Japan

December 2000

Contents

Chapter 3

Nitrogen Absorption and Desorption Characteristics over Rare earth-Iron Intermetallic Compounds

General Introduction

Metal hydrides are mainly classified to three types on the basis of the bond characters between metal and hydrogen. Intermetallic compounds such as $LaNi_5$ reversibly absorb and desorb large amounts of hydrogen under mild conditions around ambient temperature and pressure through the formation of interstitial type (metallic bonding type) metal hydrides [1]. For ionic and covalent bonding-types of metal hydrides such as LiH and $(BeH_2)_x$, the reversible hydrogen absorption and desorption can not be proceeded under the above mild conditions, since the physicochemistry is considerably different from that of the interstitial type metal hydrides. The reversible absorption and desorption of hydrogen observed on the interstitial type metal hydrides allows us the development of the hydrogen storage technique, cathode material in the Ni-H secondary battery, and so on. In addition to the reversible absorption and desorption behavior, interstitial hydrogen accommodated in the metal hydrides exists as an atomic state and it is expected to be very reactive, so that some of interstitial type metal hydrides have been found to be good hydrogenation reagents and/or catalysts [2-11].

In analogy with the metal-hydrogen system, metal nitrides are grouped into ionic bonding, covalent bonding, and metallic bonding types by the bond characters between metal and nitrogen. Among them, the rare earth-iron intermetallic compounds R_2Fe_{17} provide the interstitial type metal nitrides by heating in N_2 or a mixed gas of NH_3-H_2 [12,13]. In particular, $Sm_2Fe_{17}N_3$ has been noted as one of promising materials for high-performance permanent magnets as bonded ones [14-21]. The nitrogenation for Sm_2Fe_{17} is usually made in N_2, but this solid-gas reaction requires the much more extreme conditions of reaction pressure (~10 MPa), temperature (~ 550 °C) and time (~72 h) to proceed completely and uniformly than the nitrogenation in the NH_3-H_2 gas mixture [12,13]. In the latter case, large amounts of nitrogen can be interstitially incorporated in

the Sm_2Fe_{17} crystal lattice (x=~5) under the moderate conditions (in the mixed gas of NH_3-H_2 under atmospheric pressure at ~450 °C for ~3 h) [12,13]. As a result, the excess nitrogen (Δx) in $Sm_2Fe_{17}N_x$ (Δx=x-3) must be reversibly desorbed as N_2 down to x=3 during the annealing process by heating at ~500 °C in inert gas such as Ar to obtain the optimal nitrogen concentration for magnetic properties [12,13].

The ionic bonding type metal nitrides such as NaN_3 are commercially used as nitrogen gas generator to operate the safety bags of automobiles. Nitrogen, however, cannot be reversibly recharged due that the gas generation proceeds via the oxidative decomposition of NaN_3 (see below scheme).

$$NaN_3 \xrightarrow{KClO_4} Na_2O + 3/2N_2$$

On the contrary to NaN_3, the nitrogen absorption and desorption behavior observed on the $Sm_2Fe_{17}N_x$ indicates that the interstitial metal nitrides can absorb and desorb nitrogen through the formation of interstitial type metal nitrides in a similar manner as observed in the same type of metal hydrides. From this fact, it is expected that the interstitial metal nitrides are candidates for a novel nitrogen storage materials in a similar manner as the hydrogen storage ones. Furthermore, the nitrogen in the interstitial type metal nitrides exists in an atomic state and it is expected to be highly reactive. One can see that efficient nitrogenation process using highly reactive nitrogen atoms in these metal nitrides must be designed. The objects of this work are to develop a novel nitrogen storage technique using interstitial type metal nitrides and to construct new process for the nitrogenation reaction using the atomic nitrogen in these metal nitrides.

The thesis of this work consists of the following chapters:

In chapter 1, the nitrogenation and hydrogenation was conducted for the rare earth-iron intermetallic compounds R_2Fe_{17} (R=Y, Ce, Sm) to investigate the nitrogen absorption and desorption properties over them by heating in a NH_3-H_2 mixed gas and in H_2 one, respectively. The surface of Sm_2Fe_{17} was modified by the loading with Ru

metal, which is active for the dissociation of ammonia and molecular hydrogen. In addition, the nitrogen storage capacity was evaluated by characterizing the structure and reaction properties for these metal nitrides.

In chapter 2, the nitrogen absorption and desorption characteristics were investigated over the iron-based transition metal intermetallic compounds, viz. Laves phase-type MFe_2 (M=Ti, Zr, Nb, Mo), CsCl-type TiFe, and σ-phase VFe by heating them in the NH_3-H_2 mixed gas for nitrogenation and H_2 gas for denitrogenation. Moreover, a novel process for the nitrogenation using highly reactive nitrogen atom in the MFe_2N_x was proposed by using amorphized $TiFe_2N_x$ powders loaded with a Ru-Al_2O_3 catalyst in N_2.

In chapter 3, the nitrogen absorption and desorption properties were investigated for the rare earth-iron intermetallic compounds, RFe_2 and RFe_7, besides on the R_2Fe_{17}-type compounds. In particular, RFe_7-type compounds belong to the same type of crystal structure for the R_2Fe_{17} (R=Ce to Tb), where the Fe(6c) sites are partially deficient instead of the substitution of rare earth metal in 3a site, meanwhile Fe(6c) sites are fully occupied for the R_2Fe_{17}-type compounds. The differences on the nitrogen absorption and desorption properties between R_2Fe_{17} and RFe_7 were discussed on the basis of their structural properties.

List of Publications

1) Formation and Hydrogenation of the Nitrogen Stored in Iron-based Intermetallic Compounds

Ken-ichi Machida, Masahiro Itoh, Kazuhiro Hirose, and Gin-ya Adachi,

Chemistry Letters, 1117 – 1118 (1998).

2) Nitrogen Storage Properties based on Nitrogenation and Hydrogenation of Rare Earth-Iron Intermetallic Compounds R_2Fe_{17} (R=Y, Ce, Sm)

Masahiro Itoh, Ken-ichi Machida, Hiroharu Nakajima, Kazuhiro Hirose, and Gin-ya Adachi,

Journal of Alloys and Compounds, **288**, 141-146 (1999).

3) Nitrogenation and Hydrogenation Characteristics of Transition Metal-Iron Intermetallic Compounds

Masahiro Itoh, Ken-ichi Machida, Kazuhiro Hirose, Takao Sakata, Hirotaro Mori and Gin-ya Adachi,

The Journal of Physical Chemistry B, **103**, 9498 – 9504 (1999).

4) Nitrogen Absorption and Desorption Characteristics for $CeFe_7$ and Ce_2Fe_{17}

Masahiro Itoh, Ken-ichi Machida, Kazuhiro Hirose, and Gin-ya Adachi,

in preparation.

Chapter 1

Nitrogen Storage Property through Nitrogen Absorption and Desorption for Rare Earth-Iron Intermetallic Compounds R_2Fe_{17} (R=Y, Ce, Sm)

1.1 Introduction

Rare earth-iron intermetallic compounds, R_2Fe_{17}, provide the corresponding interstitial type metal nitrides ($R_2Fe_{17}N_x$) by nitrogenation in N_2 or NH_3-H_2 mixed gas. Usually, the nitrogenation for R_2Fe_{17} is made in N_2, but it needs the much more severe conditions of high pressure, temperature, and time than the nitrogenation in the NH_3-H_2 mixture gas. In the latter case, nitrogen can be easily absorbed in the R_2Fe_{17} crystal lattice under the more moderate reaction conditions. And then, the excess nitrogen in $R_2Fe_{17}N_x$ (x>3) is reversibly desorbed by heating in Ar atmosphere to form the $R_2Fe_{17}N_3$ compounds in a similar manner as metal hydride systems such as $LaNi_5H_x$. This behavior of nitrogen absorption and desorption has a close relation to the sites for nitrogen in the crystal lattices. Crystal structures of $Sm_2Fe_{17}N_x$ and $Y_2Fe_{17}N_x$ are shown in Figs. 1.1 [22]. The crystal structure of Sm_2Fe_{17} is classified as a Th_2Zn_{17}-type one with a space group of $R\bar{3}m$ and is formed when rare earth metals (R) are Ce, Pr, Nd, Sm, Gd and Tb. Meanwhile, the R_2Fe_{17} compounds of R = Y, Dy, Ho, Er, Tm, and Lu crystallize in another Th_2Ni_{17}-type structure (space group = $P6_3/mmc$) [22]. Buschow *et al.* [23] have concluded from neutron diffraction measurements of $Th_2Fe_{17}N_3$ with the same as the Th_2Zn_{17}-type structure that the nitrogen occupies the 9e sites represented by the space group $R\bar{3}m$ symmetry. However, the 9e sites can only accommodate three nitrogen atoms per an R_2Fe_{17} formula unit and it has also deduced from the neutron diffraction measurement of $Th_2Fe_{17}D_x$ (x=$\sim$5) that the excess nitrogen in $Sm_2Fe_{17}N_x$

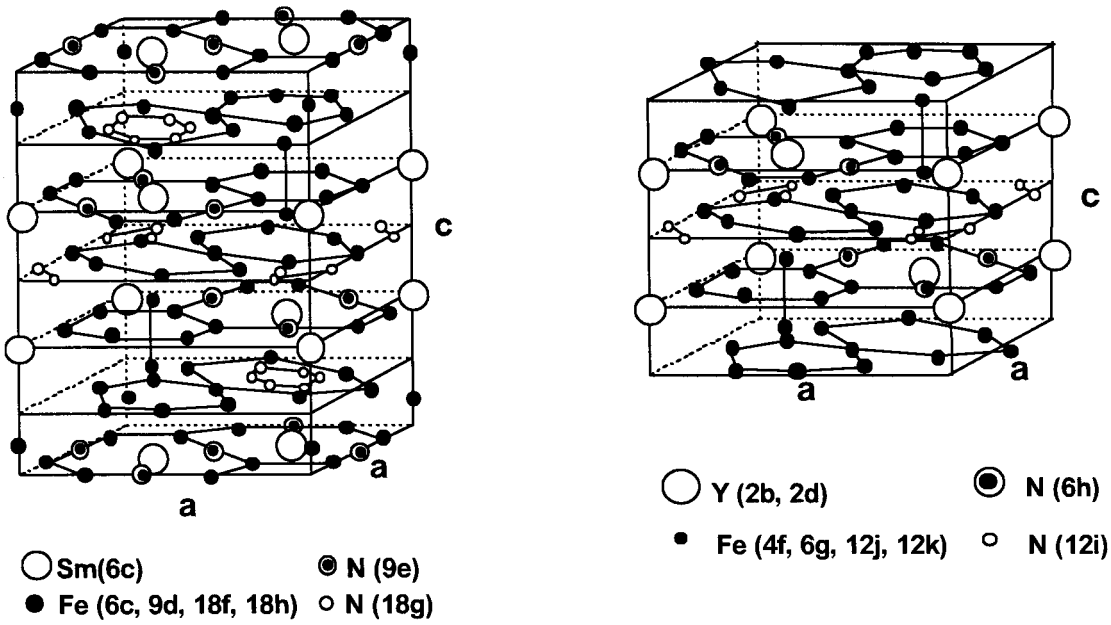

Fig. 1.1. Crystal structures of $Sm_2Fe_{17}N_x$ (left) and $Y_2Fe_{17}N_x$ (right).

(3<x<7) occupies other sites such as 18g site [23]. In the case of $Y_2Fe_{17}N_x$, the nitrogen shares 6h sites of the Th_2Fe_{17}-type crystal cell up to x=3, and the excess nitrogen occupies 12i sites [24]. Therefore, the nitrogen absorbed more than x=3 as $R_2Fe_{17}N_x$ is released down to x=3 since the nitrogen on the 9e or 6h sites is stable but not on the 18g or 12i sites. This behavior suggests that the R_2Fe_{17} compounds store large amounts of nitrogen in the crystal lattices in a similar manner as hydrogen storage materials. In addition, as the nitrogen in $R_2Fe_{17}N_x$ exists as a atomic state [24], and it is expected that the nitrogen in $R_2Fe_{17}N_x$ is considerably reactive, the nitrogen atoms stored above x=3 in the crystal lattice are regenerated as ammonia by replacing the atmosphere from Ar to H_2 in the above-mentioned treatment process for nitrogen desorption.

In this chapter, the nitrogenation and hydrogenation of R_2Fe_{17} were performed in streams of NH_3-H_2 mixture and H_2 to characterize the nitrogen absorption and desorption property based on the formation of $R_2Fe_{17}N_x$, together with composite materials, Ru/Sm_2Fe_{17}, of which Ru metal was loaded on the surface in order to promote the reactions for nitrogenation and hydrogenation. A novel nitrogen storage

technique is proposed from the discussions on the nitrogen absorption and desorption properties over R_2Fe_{17}.

1.2 Experimental

The intermetallic compounds R_2Fe_{17} (R= Y, Ce and Sm) were prepared from appropriate amounts of rare earth metal ingots or shots (>99.9 % in purity) and Fe rods (> 99.95 % in purity) by arc melting, and then annealed in He at 1100 °C for 48 h. The ingots obtained were ground into powders with a particle size below 50 μm (BET surface area=0.15-0.30 m^2/g). Further, some of Sm_2Fe_{17} was activated by the loading of Ru metal cluster particles derived from $Ru_3(CO)_{12}$ on the surface of it: After 1.0 g of the Sm_2Fe_{17} powder was impregnated with a hexane solution containing 0.06 g of $Ru_3(CO)_{12}$, the resulting composite materials were dried in N_2 at room temperature over night and heated at 300 °C in H_2 for 3 h.

The R_2Fe_{17} or Ru/R_2Fe_{17} powder (1.0 g) charged in a conventional fixed-bed quartz tube reactor (12 mm o.d.) was nitrogenated in a stream of mixed NH_3-H_2 gas (molar ratio=1:1) with a flow rate of 30ml/min at 350-450 °C for 3 h (nitrogen absorption step), followed by the subsequent hydrogenation process performed in a H_2 stream with the same flow rate at 450°C for 3 h as the absorption step. The nitrogen storage capacity of R_2Fe_{17} powders was evaluated from the difference between the nitrogen contents directly measured on a nitrogen/oxygen analyzer (Horiba, EMGA 550) for the metal nitrides before and after the nitrogen desorption ($R_2Fe_{17}N_x$ and $R_2Fe_{17}N_{x-\delta}$). The structural change was checked every step for the nitrogenation and hydrogenation treatment by measurements of powder X-ray diffraction (XRD) by a MAC Science M18XHF-SHA diffractometer using Cu Kα radiation equipped with a curved graphite monochlometer. The nitrogen species (NH_3) stripped from the metal nitrides by H_2 in the nitrogen desorption step was accumulated in a cold trap (-196 °C)

and then it was analyzed on a mass spectrometer. The amount of ammonia product was quantified by the difference between the pH values of an H_2SO_4 solution trap before and after passing gas generated from the metal nitride in the nitrogen desorption step. Nitrogen absorption and desorption properties of the Sm and Fe metals used as the starting materials were also characterized on their powders (BET surface area=~0.16 m^2 g^{-1}) by the same methods as used for R_2Fe_{17}.

The catalytic activities of ammonia decomposition over Sm_2Fe_{17}, Ru/Sm_2Fe_{17} and Fe were measured by a gas chromatograph (Shimadzu GC-8A) in a temperature range from 200 °C to 700 °C. The inlet gas composition was 5% NH_3 and He as a balance with a flow rate of 20 ml/min. The decomposition yield from NH_3 to N_2 over each powder was calculated by integrating their peak area ratio.

1.3 Results and discussion

Figures 1.2 show the typical XRD patterns measured on the powdered Sm_2Fe_{17} and Y_2Fe_{17} nitrogenated in NH_3-H_2 mixed gas at 450 °C for 3h and hydrogenated in H_2 gas at 450 °C for 3h, together with the as-obtained one. As shown in Figs 1.2b, the diffraction peaks shifted to the lower angle side than those of the obtained after the nitrogenation treatment (nitrogen absorption). These indicate that nitrogen is incorporated interstitially into their crystal lattices as accompanied with lattice expansion. After the subsequent hydrogenation (nitrogen desorption), their XRD patterns inversely shifted to the higher angle side, suggesting lattice shrinkage for desorbing nitrogen from their crystal lattices (see Figs 1.2c). A part of the $R_2Fe_{17}N_x$ compounds decomposed after the hydrogenation to α-Fe as shown in Figs. 1.2c because the resulting metal nitrides were metastable. The intensities of diffraction peaks for these intermetallic compounds were weaken and broaden with the nitrogenation treatments. The large amounts of the nitrogen incorporated into the crystal lattices

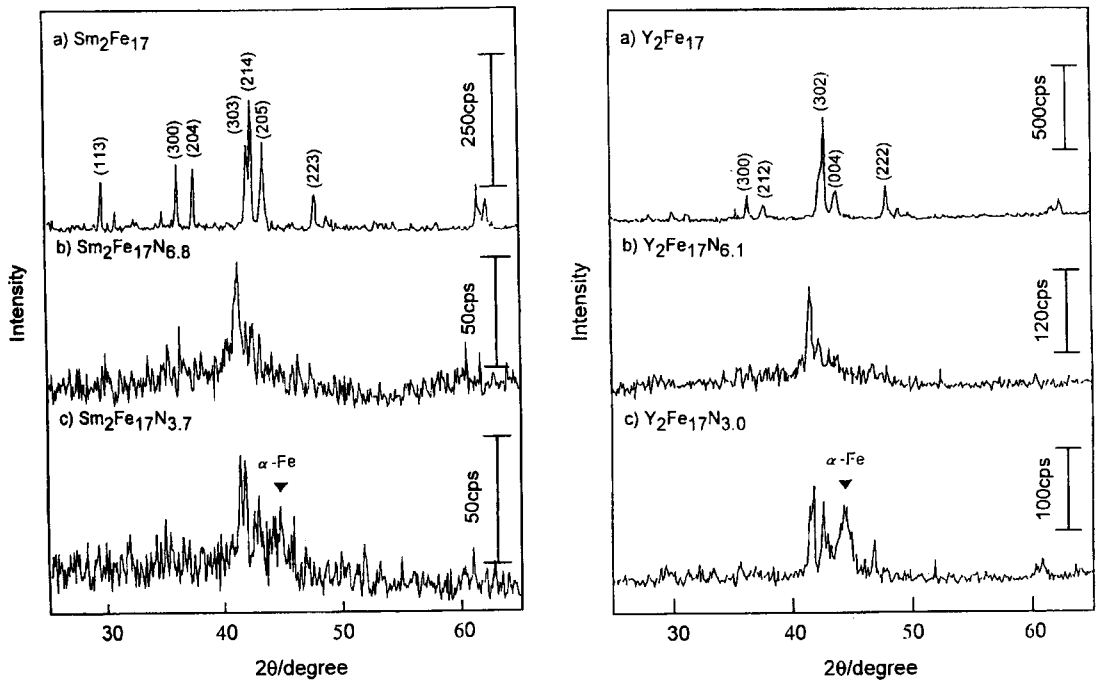

Figs. 1.2. XRD patterns of the Sm_2Fe_{17} (left) and Y_2Fe_{17} (right) powders : a) as obtained, b) nitrogenation in NH_3-H_2 mixed gas at 450 °C for 3h, and c) hydrogenation in H_2 gas at 450 °C for 3h.

lowered the crystallinity.

Mass spectra for the nitrogen species regenerated from the $Sm_2Fe_{17}N_x$ and $Y_2Fe_{17}N_x$ powders heated during reactions in H_2 at 450 °C for 3 h were shown in Figs.

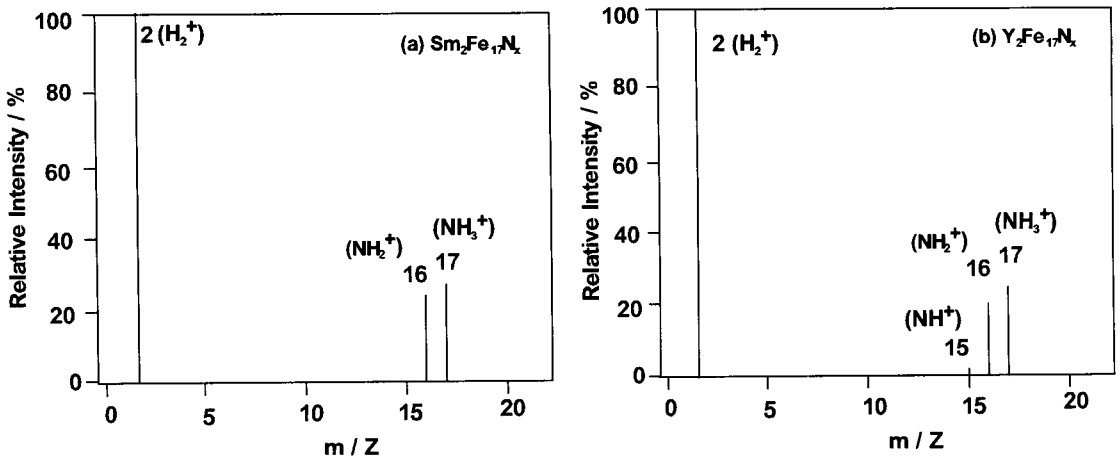

Figs. 1.3. Typical mass spectra for the nitrogen species eluted from (a) $Sm_2Fe_{17}N_x$ and (b) $Y_2Fe_{17}N_x$ powders with H_2.

1.3. The mass signals were appeared at the M/Z values of 2, 15, 16 and 17, which were

assigned to H_2^+, NH^+, NH_2^+ and NH_3^+ ion species, respectively. Since NH_3 is responsible for the fraction ion species of NH^+, NH_2^+ and NH_3^+, and H_2^+ is mainly originated from the H_2 stripping gas used here, it is concluded that the nitrogen absorbed in the R_2Fe_{17} crystal lattices is regenerated as NH_3 by stripping with H_2. In addition, the amounts of ammonia evaluated from the difference between the pH values of H_2SO_4 solution trap observed before and after the heat treatment in H_2 were in good accordance with the amount of nitrogen desorption determined directly by the nitrogen analysis for the metal nitride powders. It can be seen from these results that the nitrogen released from the $R_2Fe_{17}N_x$ powders were converted to ammonia at almost 100% of yield.

The nitrogen absorption and desorption characteristics of R_2Fe_{17}, Ru/Sm_2Fe_{17}, Sm and Fe powders observed on the nitrogenation in the NH_3-H_2 mixed gas at 350 or 450 °C for 3 h and on the hydrogenation in H_2 at 450 °C for 3 h are summarized in Table 1.1. Even for the nitrogenation at 350 °C, Ru/Sm_2Fe_{17} absorbed a significant amount of nitrogen to form $Ru/Sm_2Fe_{17}N_{4.9}$. The nitrogen content decreased down to x=2.6 after the subsequent desorption reaction. On the other hand, no Ru metal loaded Sm_2Fe_{17} powder was nitrogenated up to x=3.1 and desorbed nitrogen down to x=2.0 under the same reaction conditions. The nitrogen absorption-desorption property over Ru/Sm_2Fe_{17} was superior to that over Sm_2Fe_{17} due that the catalytic activity of Ru metal for the dissociation of NH_3 and H_2 [25]. For the nitrogen desorption step, it is considered that the hydrogen atoms diffuse into the crystal lattice and push the nitrogen in the crystal lattice out of the metal. From a calculation based on the difference of nitrogen content (Δx=2.3) between $Ru/Sm_2Fe_{17}N_{4.9}$ and $Ru/Sm_2Fe_{17}N_{2.6}$, the quantity of the nitrogen desorbed from 1 cm^3 of the metal nitride (ρ=ca.7.6 g cm^{-3}) was equivalent to 13.13 mmol of NH_3, because the atomic nitrogen stored in the crystal lattice were regenerated as NH_3 at 100% of yield in the desorption step. It is noted that this amount of the nitrogen regenerated from 1 cm^3 of the metal nitride is comparable to the storage

Table 1.1 Nitrogen absorption and desorption characteristics of R_2Fe_{17}, Ru/Sm_2Fe_{17},Sm, and Fe

Compound	Cycle number	Temp./°C [a]	Nitrogen content (x) [b]		Regenerated ammonia ($mmol/cm^3$) [c]
			After absorption	After desorption	
$Sm_2Fe_{17}N_x$	1	350	3.1	2.0	6.25
$Ru/Sm_2Fe_{17}N_x$	1	350	4.9	2.6	13.13
$Y_2Fe_{17}N_x$	1	450	6.1	3.0	17.05
$Ce_2Fe_{17}N_x$	1	450	6.6	3.7	16.96
$Sm_2Fe_{17}N_x$	1	450	6.8	3.7	17.59
	11	450	8.4	2.9	31.61
$Ru/Sm_2Fe_{17}N_x$	1	450	7.5	3.6	22.41
	11	450	8.6	2.8	36.43
SmN_x	1	350	0	0	0
	1	700	1.0	0.98	1.07
FeN_x	1	350	0.01	0	1.43
	1	450	0.14	0.01	18.39

(a) Reaction temperature of nitrogenation.
(b) Nitrogen contents were represented per chemical formula unit by determining from the nitrogen analysis data.
(c) The amount of ammonia regenerated is calculated as that nitrogen released from 1 cm^3 of metal nitride is converted into ammonia. For example, the NH_3 amount generated from 1 cm^3 of nitrogen gas container stuffed at 15 MPa is calculated to be 12.23 mmol if the N_2 gas might be converted to NH_3 at 100% of yield.

capacity of conventional high-pressure nitrogen containers charged at 15 MPa (6.12 mmol of N_2 gas per 1 cm^3 of their containers' volume). The diffusion rate of nitrogen at 350 °C in the R_2Fe_{17} crystal lattice, however, is not enough to form the metal nitrides uniformly, and the core region of R_2Fe_{17} particles has not yet completely nitrogenated only by heating for 3 h. Therefore, the complete absorption of nitrogen may need the much more time for the nitrogenation than 3 h.

The nitrogenation at 450 °C absorb the more amount of nitrogen in the R_2Fe_{17} crystal lattice than at 350 °C, due to the enhancement of diffusion rate of nitrogen and of ammonia decomposition over their surfaces. Amounts of the ammonia regenerated from the $R_2Fe_{17}N_x$ and $Ru/Sm_2Fe_{17}N_x$ powders were evaluated to be 16.96-17.59 and 22.41 mmol per 1 cm^3 of the intermetallic compounds respectively, and these values were 1.4

to 1.8 times larger than the nitrogen atom content as N_2 gas stored per unit volume of the conventional high-pressure nitrogen containers (12.24 mmol). It was not observed the obvious differences in the amounts of ammonia regeneration among the individual intermetallic compounds. It might be understood that the difference between the crystal Th_2Zn_{17}-type structure for Ce and Sm and the Th_2Ni_{17}-type structure for Y has little influence on the nitrogen storage capacities of them for the similarity in their crystal structures, and the standard enthalpy values of nitride formation are almost same as one another for the rare earth metals in this study [26].

On the other hand, since the Sm metal used as one of the starting materials was inactive for the dissociation of NH_3 even at 450 °C, only a trace of nitrogen was introduced into the crystal lattice. The formation of SmN required the higher reaction temperature of 700 °C. Fe metal also hardly reacted with NH_3 at 350 °C, although a large amount of nitrogen is incorporated into their lattices for R_2Fe_{17}. At 450 °C, however, a large amount of nitrogen was introduced in the Fe metal bulk as FeN_x, and a significant amount of NH_3 (18.39 mmol per 1 cm^3 of FeN_x) was regenerated by the subsequent hydrogenation. The XRD pattern of nitrogenated Fe metal powder was assigned according to that reported on an interstitial Fe_4N compound [27]. These results suggest that the reversible absorption and desorption of large amounts of nitrogen over R_2Fe_{17} is contributed to the combination of the Sm and Fe metals, where Sm plays a role for a high nitrogen storage ability, while Fe for ability of easy nitrogen desorption.

Figure 1.5 shows the decomposition properties of ammonia over Sm_2Fe_{17}, Ru/Sm_2Fe_{17}, and Fe powders. The surface areas of these powders are 0.15-0.30 m^2/g measured by the conventional BET method and nearly the same. The initial temperature of ammonia decomposition over Sm_2Fe_{17} powder is lower than that over the Fe powder. This result indicates that the activity for ammonia decomposition over the Sm_2Fe_{17} powder is higher than that of the Fe powder. Furthermore, ammonia was decomposed on the Ru/Sm_2Fe_{17} composite powder at a lowered temperature compared with no Ru

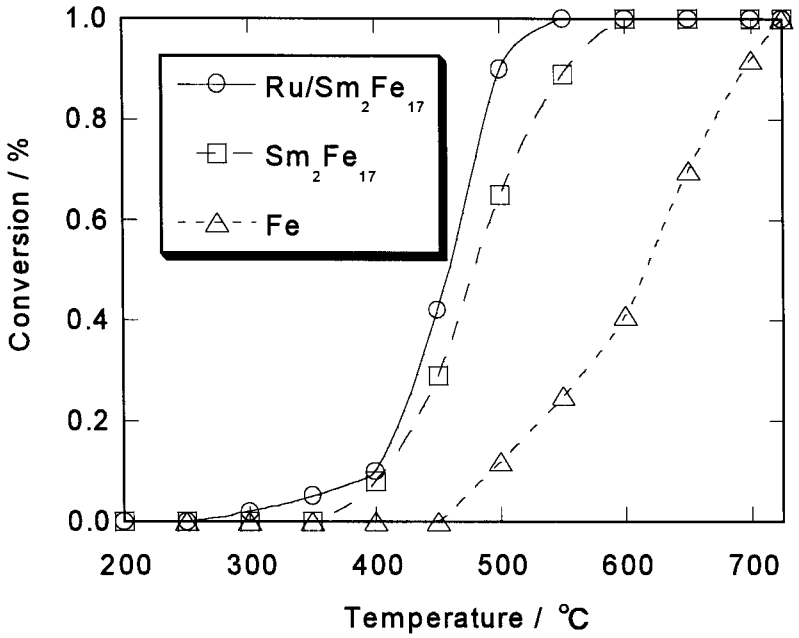

Fig. 1.4. Decomposition properties of ammonia over Sm_2Fe_{17}, Ru/Sm_2Fe_{17} and Fe powders.

metal loaded Sm_2Fe_{17} because of the high catalytic activity of Ru metal for the NH_3 dissociation and recombination [25]. The ammonia decomposition characteristics over Sm_2Fe_{17}, Ru/Sm_2Fe_{17} and Fe powders fairly agreed with their nitrogen storage properties summarized in Table 1. Since the catalytic activity of Fe metal and Fe_4N is lower than that of R_2Fe_{17} and $R_2Fe_{17}N_x$, the Fe metal cannot absorb the large amount of nitrogen compared with them even by the nitrogenation at 450 °C.

The nitrogen storage capacity of $Sm_2Fe_{17}N_x$ was increased with repeating the nitrogen absorption-desorption cycle. An amount of the ammonia regenerated from the $Sm_2Fe_{17}N_x$ and $Ru/Sm_2Fe_{17}N_x$ powders in the 11th cycle (31.61 and 36.43 mmol) was considerably higher than that in the 1st cycle (17.59 and 22.41 mmol) (see Table 1). However, the XRD pattern of $Sm_2Fe_{17}N_x$ was mixed with those of α-Fe and amorphous phases after several nitrogen absorption-desorption cycles. This finding means that a kind of composite material, FeN_x/a-(Sm, Fe)N_y, which is derived from Sm_2Fe_{17} by repeating the nitrogen absorption-desorption cycle, gives an excellent nitrogen

absorption and desorption property, as the XRD pattern of SmN has not yet been observed on the composite sample. It is concluded that the FeN_x/a-(R, Fe)N_y composite material is also highly active for the dissociation of NH_3. In the study of ammonia synthesis using rare earth intermetallics, rare earth-iron intermetallics generated the precipitation of α-Fe after the reaction of N_2-H_2 mixed gas under a pressure of 7MPa and high catalytic activity was observed over them [28]. The increase of ammonia amount obtained in 11th cycle is ascribed to the increase of the surface area due to the crack growth on the surface and decomposition of the Sm_2Fe_{17} by repeating nitrogen absorption-desorption cycle and the high activity of ammonia dissociation over the FeN_x/a-(R, Fe)N_y composite materials.

Schematic models for the nitrogen absorption and desorption steps took place on a $Ru/Sm_2Fe_{17}N_x$ or $Ru/Sm_2Fe_{17}N_{x-\delta}$ particle are shown in Figs. 1.5. Nitrogen is reversibly absorbed and desorbed by repeating the nitrogenation and hydrogenation cycle. A novel nitrogen storage technique can be designed by using the interstitial type metal nitrides.

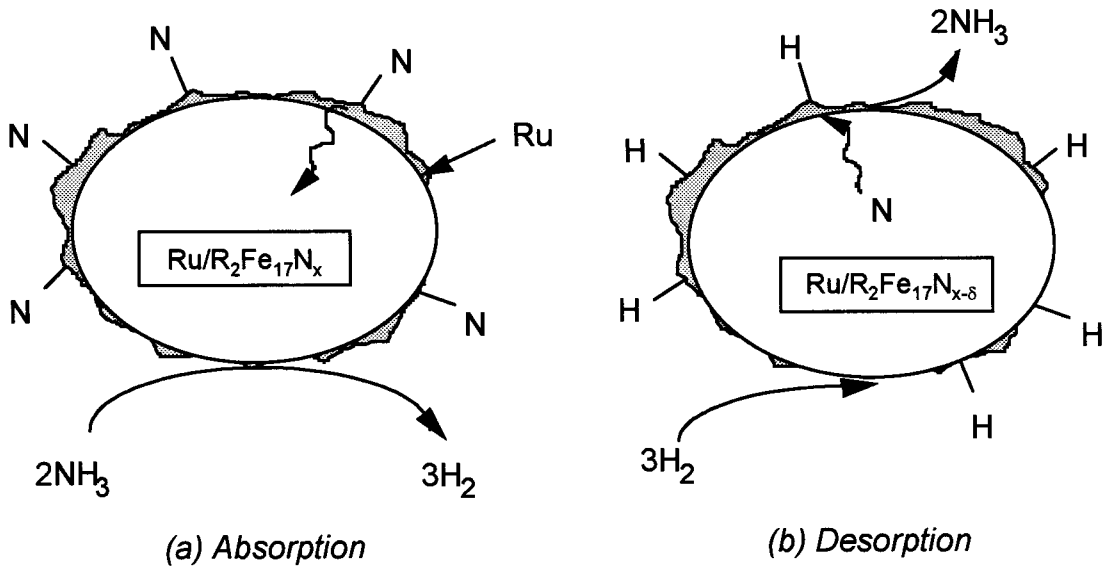

Fig. 1.5. Schematic models of the nitrogen absorption and desorption steps over the Ru/R_2Fe_{17}.

1.4 Conclusions

Rare earth-iron intermetallic compounds R_2Fe_{17} (R=Y, Ce and Sm) absorb and desorb nitrogen reversibly through the nitrogenation by heating in the mixed gas of NH_3-H_2 and denitrogenation by heating in H_2 gas. The nitrogen storage capacities per unit volume through absorption-desorption for these samples are superior to those of conventional high pressure nitrogen containers charged at 15 MPa. More improvement for the nitrogen storage capacity of R_2Fe_{17} than the above one is attained by loading the Ru metal on their powder surface because of the acceleration for the nitrogenation and hydrogenation. The atomic nitrogen incorporated in the compounds is regenerate as ammonia in the nitrogen desorption step at almost 100% of yield due to the high reactivity of atomic nitrogen. In addition, the nitrogen storage capacity of $Sm_2Fe_{17}N_x$ is increased with repeating the nitrogen absorption/desorption cycle due to the formation of FeN_x/a-(Sm, Fe)N_y fine particle composites.

Chapter 2

Hydrogenation and Nitrogenation Characteristics for Iron-based Transition Metal Intermetallic Compounds

2.1 Introduction

Intermetallic compounds such as $LaNi_5$ have interstitial vacancies to accommodate small atoms such as hydrogen, nitrogen, and carbon. These compounds form the interstitial-type compounds by hydrogenation, nitrogenation, and carbonation. In particular, interstitial type metal hydrides can reversibly absorb and desorb large amounts of hydrogen under mild conditions. In chapter 1, it was elucidated that rare earth–iron intermetallic compounds R_2Fe_{17}, which have interstitial site vacancies, can absorb large amounts of nitrogen by heating in a flow of NH_3–H_2 mixed gas and the nitrogen incorporated into the crystal lattice is reversibly released by the subsequent heat treatment in a flow of H_2 gas. This facts indicate that rare earth-iron intermetallic compounds behave as so-called "nitrogen storage materials". Indeed, the density of the nitrogen stored in these compounds is 2-3 times higher than those for the conventional nitrogen containers charged at 15 MPa per unit volume.

On the other hand, it is known well that intermetallic compounds between transition metals such as TiFe and $TiMn_{1.5}$ are good hydrogen storage materials [29, 30]. These compounds have enough vacant sites in crystallographic cell to accommodate hydrogen, so that it is expected that nitrogen can be also reversibly absorbed and desorbed on them like as observed on R_2Fe_{17}.

In this chapter, a series of the Laves-phase MFe_2 (M=Ti, Zr, Nb, and Mo) and AB-type M'Fe (M=Ti and V) compounds were prepared, and the nitrogen absorption and desorption properties were characterized by heating them in the NH_3-H_2 mixed gas and H_2 gas, respectively. Furthermore, the direct conversion from molecular nitrogen to

ammonia over the amorphous-like $TiFe_2N_x$ was conducted by loading the Ru/Al_2O_3 catalyst on the surface.

2.2 Experimental

The MFe_2–type compounds were prepared by arc-melting appropriate amounts of transition metal shots or ingots (>99% in purity) and Fe wire (>99.9% in purity) together in Ar (99.999% in purity). The ingots of intermetallic compounds obtained were annealed in He (99.999% in purity) at 1100 °C for 48 h and then they were crushed and pulverized into fine particles with diameters below 50 μm. The M'Fe-type compounds were prepared in the same way. A part of the $TiFe_2$ powder were impregnated with $Ru_3(CO)_{12}$ and $Al(C_2H_5)_3$ in their n-hexane solutions as precursors to prepare the $Ru/Al_2O_3/TiFe_2$ composite powder: Al_2O_3 was initially formed on the surface of the $TiFe_2$ particles by the oxidative decomposition of $Al(C_2H_5)_3$ in air at room temperature after impregnating, while Ru metal was loaded *via* the decarbonylation of the $Ru_3(CO)_{12}$ metal cluster compound as impregnated on the $Al_2O_3/TiFe_2$ composite particles by heating in H_2 at 300 °C. The procedural details were described elsewhere [31, 32].

The intermetallic compounds prepared in this study were identified on the basis of the powder X-ray diffraction measurements by a MAC Science M18XHF-SHA diffractometer using Cu Kα radiation equipped with a curved graphite monochlometer. In addition, selected area electron diffraction measurements were performed with a Hitachi H-800 transmission electron microscope operated at 200 kV. Specific surface area values for the powdered intermetallic compounds were measured by a conventional BET method, together with those of Ti and Fe powders.

Each powder of MFe_2, M'Fe, Ti, and Fe was charged in a conventional fixed-bed quartz reaction tube (12 mm o.d.), and the nitrogenation (nitrogen absorption) reactions were performed at 450-500 °C in a stream of the NH_3-H_2 mixed gas (molar ratio =1:1)

or N_2 gas with a flow rate of 30 ml/min. The hydrogenation (nitrogen desorption) reaction was carried out at 450 °C in a H_2 gas stream with the same flow rate. Their nitrogen storage properties were valuated from the differences between the nitrogen contents before and after the hydrogenation. The nitrogen content was determined by a nitrogen/oxygen analyzer (Horiba, EMGA 550). Nitrogen species eluted from the metal nitrides in the hydrogenation step were collected in a liquid nitrogen trap and analyzed on a mass spectrometer.

Catalytic activity of $TiFe_2$ and Fe for ammonia decomposition was estimated by monitoring the integrated peak intensity ratio between NH_3 and its degradation product (N_2) measured on a gas chromatograph (Shimadzu GC-8A) in a temperature range of 350-700 °C. The inlet gas composition was 5% NH_3 and He was used as a balance with a flow rate of 20 ml/min.

2.3 Results and discussion

2.3.1 Amorphous-like modifications induced by nitrogen absorption

From the XRD measurements, it was confirmed that all the intermetallic compounds prepared in this study were formed in a single phase except for the case of TiFe. The XRD patterns of $TiFe_2$, $NbFe_2$, and $MoFe_2$ were assigned to the C14 hexagonal Laves-phase structure while that of $ZrFe_2$ to the C15 cubic Laves-phase one. Figure 2.1 shows the XRD patterns for the respective $TiFe_2$ powders as nitrogenated at various temperatures (350-700 °C) in the NH_3-H_2 mixed gas for 3 h and subsequently hydrogenated at 450 °C in H_2 gas for 3 h, together with the virgin $TiFe_2$. As shown in Fig. 1b, the diffraction peaks for the $TiFe_2$ powder nitrogenated at 350 °C shifted to the lower angle side than that of the virgin specimen. This indicates that nitrogen was shared the interstitial sites to expand the crystal lattice. The lattice parameters for the $TiFe_2$ and $TiFe_2N_{0.53}$ (nitrogenated at 350 °C) compounds were determined by the least squares method as follows: a=4.793 and c=7.822 Å: a=4.820 and c=7.835 Å,

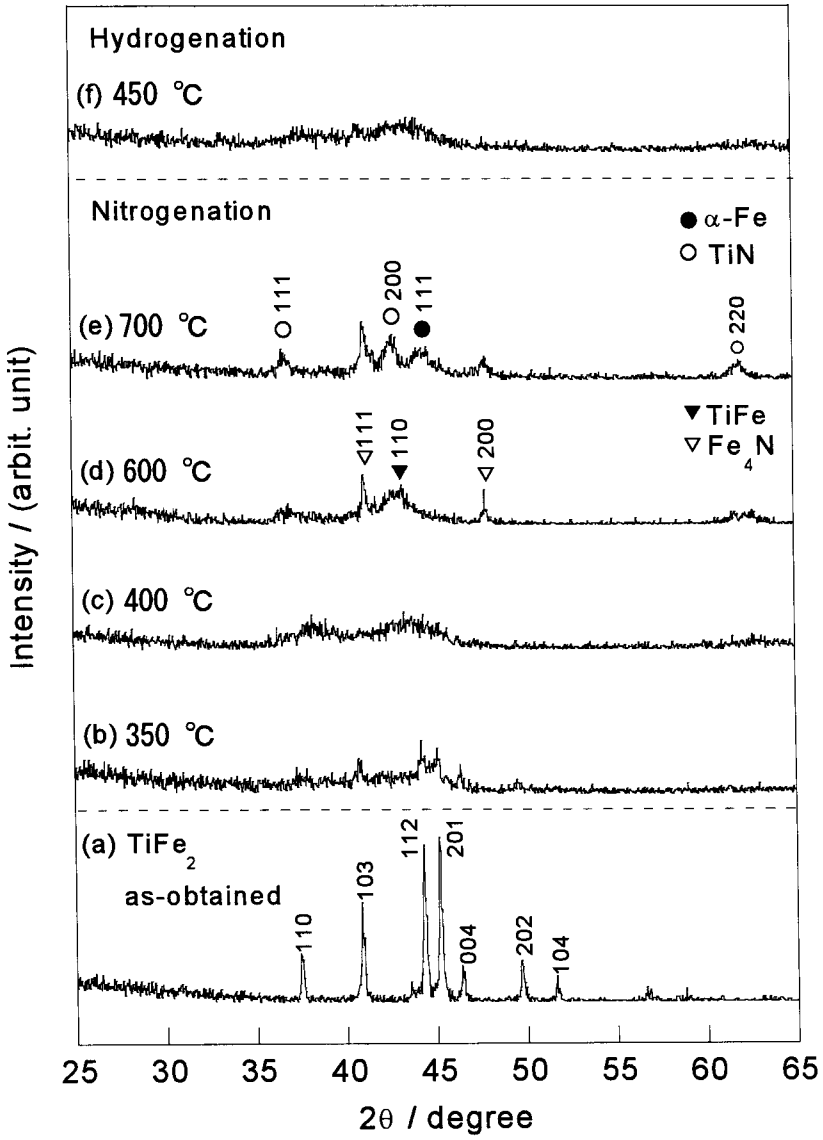

Fig. 2.1. X-ray diffraction patterns observed on the $TiFe_2$ powder nitrogenated at various temperatures (350-700 °C) in NH_3-H_2 mixed gas for 3 h (b-e) and hydrogenated in H_2 gas at 450 °C for 3 h (f), together with the as-obtained one (a). The diffraction patterns for the nitrogenated and hydrogenated $TiFe_2$ are shown below and above dashed line, respectively.

respectively. On the other hand, the $TiFe_2$ powder as nitrogenated at 400 °C absorbed nitrogen up to $TiFe_2N_{1.44}$ and only provided flattened broad XRD peaks. This fact suggests that the crystalline $TiFe_2$ transforms into the amorphous-like one caused by incorporating large amount of nitrogen into the crystal lattice. This amorphous-like

structure was maintained after the successive hydrogenation at 450 °C for nitrogen desorption step (see Fig. 2.1f). Such amorphization also takes place for the $Sm_2Fe_{17}N_{9.9}$ compound as reported by Köeninger *et al.* [33], but the resulting amorphous-like material is recrystallized to form the α-Fe phase by the hydrogenation at 450 °C. The nitrogenation at 600 ° C resulted in the decomposition of the $TiFe_2$ compound, and additional XRD patterns assigned to Fe_4N and TiFe appeared. Further decomposition occurred during the nitrogenation at 700 °C to produce TiN, Fe_4N, and α-Fe phases. Therefore, the decomposition of $TiFe_2$ during nitrogenation is elucidated to take place according to the following scheme:

$$TiFe_2 \xrightarrow{in\ NH_3\ 600^\circ C} TiFe, Fe_4N \xrightarrow{in\ NH_3\ 700^\circ C} TiN, Fe_4N, Fe$$

Figures 2.2a and b show selected-area electron diffraction patterns for the crystalline and amorphous $TiFe_2$, respectively. The net pattern shown in Fig. 2a was consistently indexed as that of $[\bar{3}\ \bar{1}\ \bar{2}\ \bar{1}]$ zone axis pattern of $TiFe_2$ with the C14 structure (see Fig. 2.2c). On the contrary, the $TiFe_2$ specimen nitrogenated in NH_3-H_2 at 450 °C did not show any obvious net pattern and instead a broad halo pattern composed of diffuse rings appeared which was characterized as the amorphous-like $TiFe_2$ phase (see Fig. 2.2b).

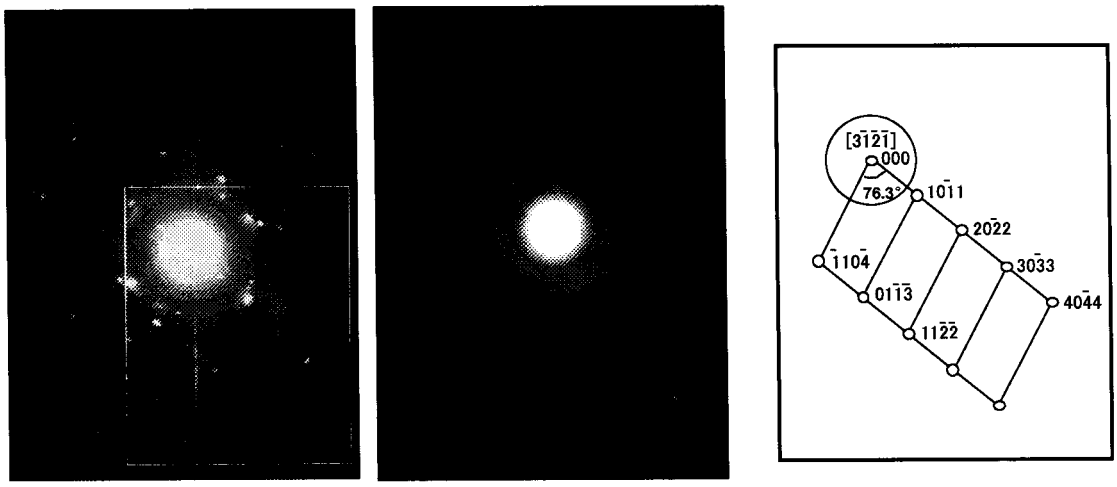

Figs. 2.2. Selected area electron diffraction patterns for (a) the crystalline $TiFe_2N_{0.53}$, (b) amorphous-like $TiFe_2N_{1.44}$, and (c) indexed key diagram for the diffraction pattern shown in (a).

Therefore, one can see that the electron diffraction patterns obtained are entirely consistent with the flattened broad profiles recorded on the XRD measurements.

Similar amorphization was observed in the C14 and C15 Laves-phase compounds such as $ZrFe_2$, $NbFe_2$, and $MoFe_2$ during the nitrogenation at 450 °C. These flattened XRD patterns suggest that the Laves-phase compounds are easily amorphized by the nitrogenation, although no hydrogen-induced amorphization has been reported on them [34]. For the hydrogen-induced amorphization observed on the C15 Laves-phase AB_2 compounds, the atomic radius ratio between the A and B elements is the most critical factor to determine whether such amorphization takes place or not [35]. The amorphization occurs only in the C15 Laves-phase compounds with the atomic radius ratios between the A and B elements (R_A/R_B) above 1.37. An ideal R_A/R_B value is 1.225 over all the Laves-phase compounds, but most of them are not in such ideal ratio value. Therefore, the crystalline Laves-phase compounds are usually stabilized by enlarging and contracting atomic radii for the individual A and B elements. The R_A/R_B value above 1.225 results in a lower stability of the Laves-phase structure, and the strained crystalline phase are consequently forced to collapse and transformed into such amorphous phase by the insertion of hydrogen into their lattices. The crystal structures for the Laves-phase compounds consist of quite analogous layered networks. They are classified into C14 $MgZn_2$-, C15 $MgCu_2$-, and C36 $MgNi_2$-types by the stacking manner of layered networks. The lattice hydrogen absorbed in the C14 Laves-phase compounds occupies the tetrahedral sites surrounded by A2B2 (two A metals and two B metals), A1B3, and B4 as well as those in the C15 Laves-phase ones [36]. It is assumed that the amorphization induced by nitrogenation can be discussed in term of the R_A/R_B value in a manner similar to the hydrogen-induced amorphization. The respective R_A/R_B values for the $TiFe_2$, $ZrFe_2$, $NbFe_2$, and $MoFe_2$ are calculated to be 1.12, 1.24, 1.14, and 1.10 by using Goldschdmit's atomic radius, and the degrees of deviation from the ideal value (1.225) for these compounds ($|\Delta R_A/R_B|$=0.015-0.125) are smaller than those observed in

the hydrogen-induced amorphization. Although the R_A/R_B value for $ZrFe_2$ is 1.24, which is responsible for its quasi-ideal Laves-phase structure and is never amorphized by hydrogenation, the nitrogenation, surprisingly, induces the amorphization. This fact indicates that the insertion of nitrogen atoms into the crystal lattice more readily induces the amorphization than that of hydrogen owing to the larger size of nitrogen atom than that of hydrogen one.

Figure 2.3a shows the XRD pattern for the virgin TiFe. It was assigned to the CsCl-type structure and an unknown phase. The crystalline TiFe did not be transformed into such amorphous-like one even after the nitrogenation (see Fig. 2.3b). The nitrogen

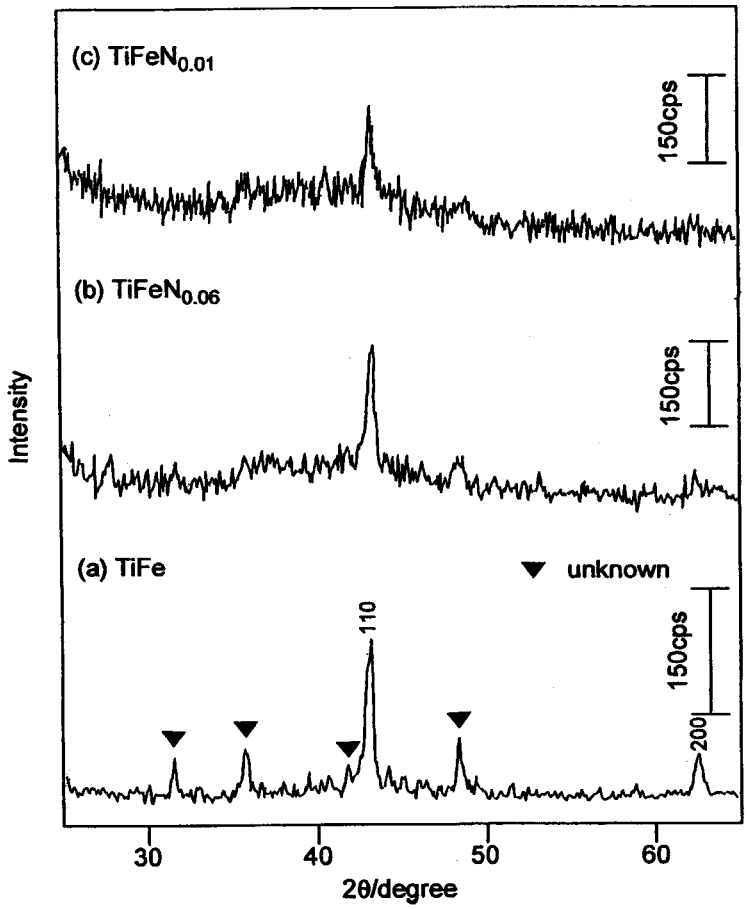

Fig. 2.3. X-ray diffraction patterns for the TiFe powders: (a), as obtained; (b), nitrogenated in NH_3-H_2 mixed gas at 450 °C for 3 h; and (c), hydrogenated in H_2 gas at 450 °C for 3 h.

content for TiFe after the nitrogenation was negligible because of the low nitrogenation rate of TiFe. This tendency is similar to hydrogenation of it [29]. In the case of VFe, however, a large amount of nitrogen was incorporated into the crystal lattice by the nitrogenation. The XRD peaks as assigned to the CrFe-type structure with tetragonal symmetry were flattened after the nitrogenation. It is presumed that the nitrogen atoms are incorporated into the tetrahedral sites surrounded by randomly or orderly occupied V and Fe atoms in the crystal lattice of CrFe-type structure [37]. These structural modifications observed on the MFe_2 and VFe indicate that the interstitial site in their crystal lattices for nitrogen occupation are too small to retain the crystalline phase, so that the nitrogen-induced amorphization more widely occurs over the intermetallic compounds compared with the hydrogen-induced one.

2.3.2 Nitrogen absorption-desorption property

Figure 2.4 shows time dependence of the heat treatments on the nitrogen content

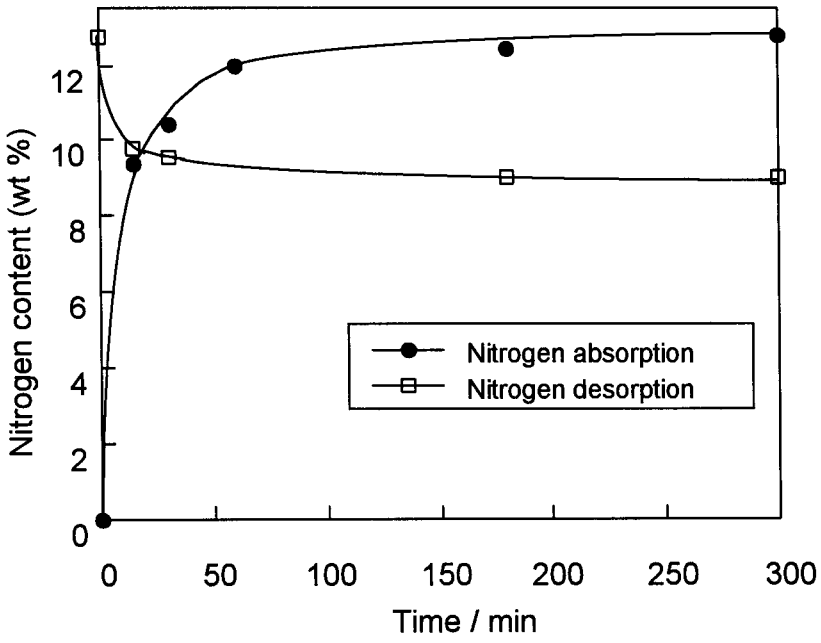

Fig. 2.4. Time dependence of nitrogen absorption and desorption observed on the $TiFe_2$ powder. (a) nitrogenation in NH_3-H_2 mixed gas at 450 °C, (b) denitrogenation in H_2 gas at 450 °C.

of $TiFe_2$ for the nitrogen absorption and desorption processes in NH_3-H_2 and H_2 at 450 °C, respectively. The nitrogen contents of $TiFe_2$ in the absorption and desorption reaction steps were almost saturated at the heating time for 60 min. These results suggest that the nitrogenation and hydrogenation reaction at 450 °C for 3h are sufficient to achieve such equilibrium nitrogen contents over the $TiFe_2$ powder with particle diameter of 50 μm. By postulating the nitrogen absorption obeys a parabolic time law, Uchida *et al.* proposed an equation for the nitrogen diffusion to the bulk represented as [38, 39],

$$x = R\{t \exp(-A/kT)\}^{1/2} \qquad (2.1)$$

where x is the nitrogen concentration, A the activation energy for diffusion, k the Boltzmann constant, T the absolute temperature, and R the temperature-independent constant. Since the nitrogenation and denitrogenation reactions obey the Eq. 2.1 below the reaction time of 30 min, the activation energy of the nitrogen diffusion was calculated from an Arrhenius plot for the temperature dependence of slope $d(x^2)/dt$ *vs.* the reciprocal of heating temperature to be 116.3 kJ/mol in the temperature range

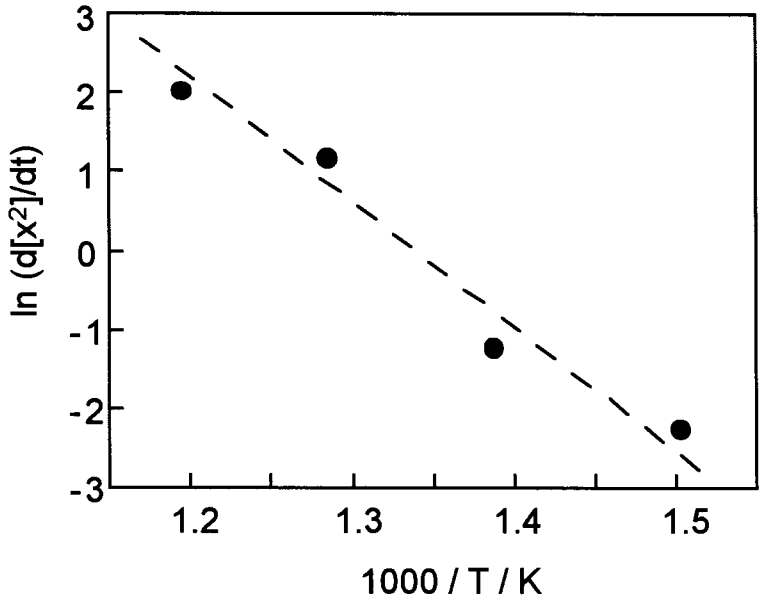

Fig. 2.5. Arrhenius plot of the nitrogen absorption rate of $TiFe_2$ in NH_3-H_2.

between 350 and 500 °C (see Fig. 2.5).

Figure 2.6 shows the typical mass spectrum observed on gaseous species eluted from $TiFe_2N_x$ during the hydrogenation. The mass signals at the m/z values of 2, 15, 16, and 17 were assigned to H_2^+, NH^+, NH_2^+, and NH_3^+ ion species respectively. The H_2^+ ion is derived from the elution gas of H_2 used here. Amounts of the ammonia products were evaluated from the differences between the pH values of H_2SO_4 solution trap before and after hydrogenation, and the resulting values were in good accordance with the ammonia amounts evaluated from the decreases in the nitrogen contents of the

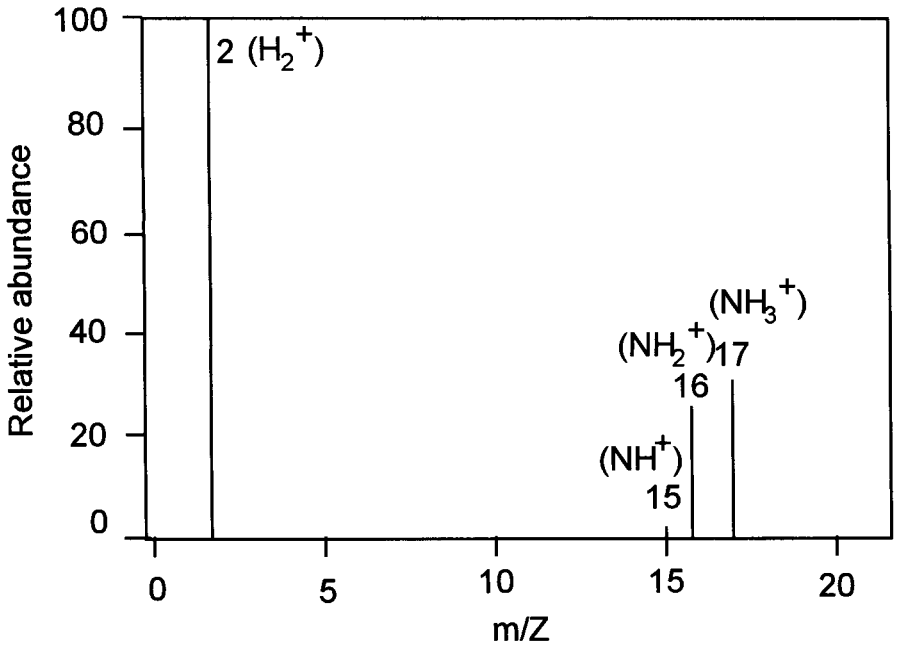

Fig. 2.6. Typical mass spectrum for the nitrogen species generated from the $TiFe_2N_x$ in the nitrogen desorption step.

hydrogenated sample directly determined by the nitrogen analysis. This result indicates that most of the nitrogen desorbed from the metal nitride is converted to ammonia in the desorption step owing to the high reactivity of atomic nitrogen.

The nitrogen absorption-desorption properties of MFe_2, M'Fe, Ti, and Fe were summarized in Table 2.1. Nitrogenation and hydrogenation treatments were performed by heating in NH_3-H_2 and in H_2 at 450 °C for 3 h, respectively. The specific surface area

Table 2.1. Nitrogen absorption and desorption characteristics of MFe_2, M'Fe, Ti, and Fe nitrogenated in the NH_3-H_2 mixed gas

metal nitride	cycle number	nitrogen content (x)		regenerated ammonia [a] (mmol/cm^3 M.N.)
		nitrogenated	hydrogenated	
$TiFe_2N_x$	1	1.48	0.93	26.25
	11	1.50	0.94	26.60
$ZrFe_2N_x$	1	1.74	1.28	19.64
$NbFe_2N_x$	1	1.76	1.16	25.17
$NbFe_2N_x$	1	0.70	0.34	15.98
$VFeN_x$	1	0.85	0.63	15.00
$TiFeN_x$	1	0.06	0.01	3.10
TiN_x	1	0	0	0
FeN_x	1	0.14	0.01	18.3

a) The amount of ammonia regenerated is calculated as that nitrogen released from 1 cm^3 of metal nitride is converted into ammonia.

values of the powdered samples used here are nearly same as one another (0.15-0.30 m^2 g^{-1}). Among them, the Laves-phase compounds,$TiFe_2$, $ZrFe_2$, $NbFe_2$, and $MoFe_2$ showed good nitrogen absorption-desorption properties *via* the transformation into the amorphous-like phases as shown in Figs. 2.1 and 2.2. The $TiFe_2$ compound interstitially absorbed large amounts of nitrogen into the disordered lattice up to $TiFe_2N_{1.48}$ and, by the subsequent hydrogenation, the interstitial nitrogen was desorbed down to $TiFe_2N_{0.93}$. From the difference of nitrogen content (Δx=0.55) between $TiFe_2N_{1.48}$ and $TiFe_2N_{0.93}$, the quantity for the nitrogen desorption per 1 cm^3 of the metal nitride (ρ=*ca.* 6.86 g cm^{-3}) was calculated to 26.25 mmol of NH_3, because the atomic nitrogen stored in the host lattices was regenerated as NH_3 at about 100% yield in the hydrogenation process. It is noted that the storage capacity of $TiFe_2$ greatly exceeds that of the conventional nitrogen container charged at 15MPa per unit volume. The amount of the ammonia

product from 1.0 cm^3 of the nitrogen gas container is equivalent to 12.2 mmol of NH_3 if the N_2 might be converted to NH_3 in 100% of yield. The $NbFe_2$ and $ZrFe_2$ compounds also absorbed large amounts of nitrogen, which were comparable to that for the $TiFe_2N_x$ one. Meanwhile, the amount of the nitrogen absorption for $MoFe_2$ was smaller and the resulting quantity of ammonia (15.98 mmol) was somewhat less than those for other Laves-phase compounds. Although the nitrogen absorption property is influenced by the factors such as the crystal structure, the nitrogen diffusion in the crystal lattices, and the catalytic activity of the surface metals, the standard formation enthalpy of metal nitride should be considered as the additional factor in this case: The enthalpy value of MoN (-92 kJ mol^{-1}) is very small compared with those for TiN (-338.1 kJ mol^{-1}), ZrN (-370 kJ mol^{-1}), and NbN (-235.1 kJ mol^{-1}).

In addition, the MFe_2 compounds showed good stability for the nitrogen absorption-desorption cycle. After the 11th nitrogen absorption-desorption cycle, the metal nitride system of $TiFe_2N_{1.50}$ (as nitrogenated) and $TiFe_2N_{0.94}$ (as hydrogenated) regenerated 26.60 mmol of NH_3 per 1cm^3 of the metal nitride. This amount is almost same as that of the 1st cycle (26.25mmol). The XRD measurements revealed that the structure of $TiFe_2N_x$ was still amorphous-like after 11th cycle. Similar behaviors were observed in the other MFe_2 compounds. Therefore, the Laves-phase MFe_2 intermetallic compounds can incorporate a large amount of nitrogen in their amorphous-like host lattices.

The CsCl-type compound TiFe hardly absorbed nitrogen, so that the resulting amount of ammonia product was only 3.1 mmol per 1cm^3 of the metal nitride, although this compound can absorb a large amount of hydrogen. The TiFe compound has been investigated also as a catalyst for ammonia synthesis. Schwab *et al.* [40] have reported that the special pretreatment made by cycling the hydrogenation and dehydrogenation for TiFe is necessary for the formation of $TiFeN_x$ on nitrogenation in NH_3. Indeed, Kirch *et al.* [41] have reported that the Fe/TiN composite materials of which the Fe

metal are highly dispersed in the TiN matrix *via* the decomposition of TiFe by nitrogenation show high activity for ammonia dissociation. On the other hand, VFe reversibly absorbed and desorbed a large amount of nitrogen, and the amount of ammonia product was 15.0 mmol per $1cm^3$ of the metal nitride. For the TiFe compound, it is considered that the nitrogen atoms incorporated share the octahedral sites formed by two Fe metals and four Ti metals in a manner similar to hydrogen atoms [42]. Meanwhile, the structure of VFe is classified as the σ-CrFe-type structure which is similar to β-U-type one [43]. The crystal structure of β-U consists of layered networks [44], and the isostructural analogous compounds such as VFe have many interstitial vacancies to incorporate nitrogen. It is expected that the nitrogen absorbed is located on such interstitial sites.

A large amount of ammonia product (18.3 mmol) was observed on Fe through the nitrogenation and hydrogenation. This high capacity for the nitrogen storage is also due to the formation of interstitial metal nitride. The nitrogen absorbing property of Ti, Nb, or Mo was very poor and no interstitial metal nitride phase was judged from the XRD measurements after nitrogenation. The XRD pattern for Fe after the nitrogenation consists of two phases assigned to Fe and Fe_4N. It is found that the nitrogen absorption rate of Fe powder (50 μm) is slower than that for the $TiFe_2$ of similar particle diameter. However, the resulting Fe_4N phase was easily denitrogenated to α-Fe by the hydrogenation in H_2 gas at 450 °C.

Figure 2.7 shows the decomposition properties of ammonia over the $TiFe_2$ and Fe powders. A drastic change in the conversion from ammonia to molecular nitrogen was observed on $TiFe_2$ in a temperature range between 425 and 450 °C (0.5% at 425 °C to 12% at 450 °C). Meanwhile, Fe provided a steep increase in the higher temperature region (3% at 500 °C to 26% at 550 °C). This result indicates that the catalytic activity for the ammonia dissociation over $TiFe_2$ is higher than that over Fe, and is responsible for the large amount of nitrogen absorption for $TiFe_2$ as summarized in Table 1. Since

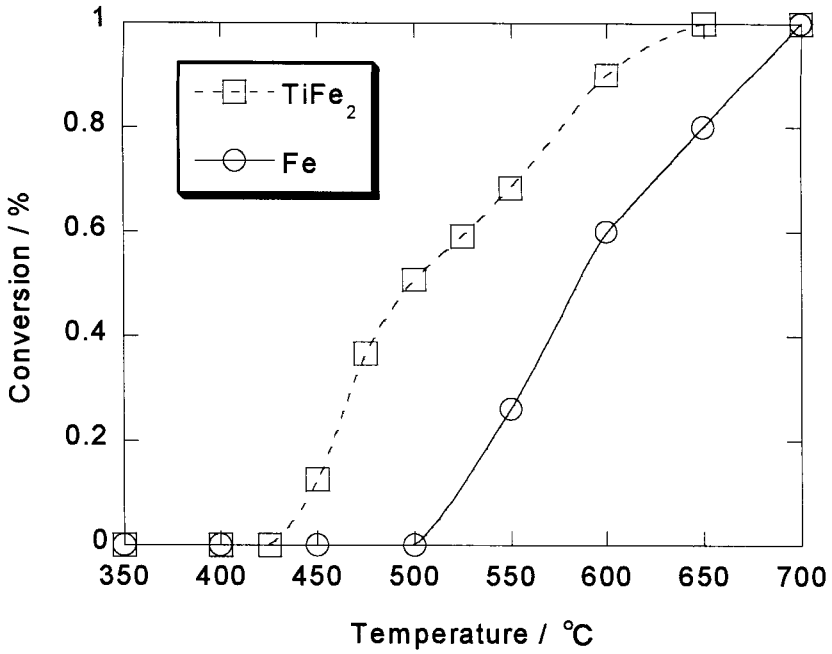

Fig. 2.7. Catalytic activity for dissociation of ammonia over the $TiFe_2$ and Fe powders.

the catalytic activity of Fe for the ammonia dissociation is lower than that of $TiFe_2$, Fe cannot be completely nitrogenated under this experimental condition, and the longer heating time is needed for the complete formation of Fe_4N.

When the molecular nitrogen is used as a nitrogen source instead of ammonia, the amount of nitrogen absorption for $TiFe_2$ decreased due to the high bond energy of N≡N. Aiming at promoting the catalytic activity of intermetallic compounds for the dissociation of molecular nitrogen, the Ru/Al_2O_3 catalyst as active for the dissociation and adsorption of molecular nitrogen was loaded on the surface of the $TiFe_2$ particles. The amounts of ammonia product for the unloaded $TiFe_2$ and loaded $Ru/Al_2O_3/TiFe_2$ powders are summarized in Table 2.2. The $Ru/Al_2O_3/TiFe_2$ composite powder absorbed the more amount of nitrogen compared with the unloaded one. The resulting metal nitride $Ru/Al_2O_3/TiFe_2N_{0.33}$, however, scarcely desorbed nitrogen in the following hydrogenation. It was found from the XRD measurements that both the $TiFe_2N_{0.1}$ and $Ru/Al_2O_3/TiFe_2N_{0.33}$ powders were still in the crystalline state even after nitrogenation.

Table 2.2. Nitrogen absorption and desorption characteristics for no loading and loading Ru/Al_2O_3 on the surface of crystalline and amorphous $TiFe_2$

metal nitride	cycle number	nitrogen content (x)		regenerated ammonia ($mmol/cm^3$ M.N.)
		Nitrogenated	hydrogenated	
(A) nitrogenated in the N_2 gas at 500 °C for 3 h				
c-$TiFe_2N_x$*	1	0.10	0.10	0
a-$TiFe_2N_x$*	1	1.14	1.14	0
Ru/Al_2O_3/ c-$TiFe_2N_x$	1	0.33	0.33	0
Ru/Al_2O_3/ FeN_x	1	0	0	0
Ru/Al_2O_3/ a-$TiFe_2N_x$	1	1.57	1.51	2.57
	2	1.60	1.55	2.14
	5	1.72	1.67	2.14
(B) nitrogenated in the NH_3-H_2 mixed gas at 450 °C for 3 h				
Ru/Al_2O_3/ a-$TiFe_2N_x$	1	1.75	1.44	13.6

* c-$TiFe_2$ and a-$TiFe_2$: crystalline and amorphous $TiFe_2$, respectively.

It is presumed that the nitrogen atom incorporated in the stable tetrahedral sites surrounded by Ti2Fe2 atom units in such low nitrogen concentration region and can not be released owing to the strong interaction between the nitrogen atom and its incorporated site. Therefore, once the $Ru/Al_2O_3/TiFe_2$ composite material is nitrogenated by heating in NH_3-H_2 to be amorphized, the subsequent denitrogenation allows us to regenerate ammonia by desorption of excess nitrogen stored in the amorphized lattice.

The pretreated Ru/Al_2O_3/a-$TiFe_2N_x$ reversibly absorbed and desorbed nitrogen even though molecular nitrogen was used as the nitriding source, providing 2.57 mmol of ammonia per $1cm^3$ of the metal nitride. Meanwhile, a-$TiFe_2$ with no loading catalyst was hardly nitrogenated under the same condition. Furthermore, the Ru/Al_2O_3/Fe composite powder as prepared from the Fe powder according to the same procedure for

$Ru/Al_2O_3/TiFe_2$ was not nitrogenated in N_2 and never produced any ammonia by the subsequent hydrogenation. These results mean that the amorphous-like phase is essential for their reversible nitrogen absorption and desorption and the Ru/Al_2O_3 catalyst plays a significant role in the dissociation of N≡N bond.

Table 2.3. Determination of The Ammonia Product from the Ru/Al_2O_3/ a-$TiFe_2N_x$ Composite Powder as Listed in Table 2

analysis	hydrogenation		generated ammonia ($\mu mol/cm^3$ of M.N.)[a)]
	before	after	
pH value (H_2SO_4 aq.)	2.52	10.09	324

a) Amount of ammonia product is evaluated from changes of the pH value of H_2SO_4 aqueous solutions before and after introducing H_2 elution gas from the metal nitride.

The Ru/Al_2O_3/a-$TiFe_2$ composite material maintained good stability against the ammonia synthesis cycle. In the 5th cycle, the amount of ammonia product was evaluated from the difference between the nitrogen contents for the nitrogenated and hydrogenated powders to be 2.14 mmol per $1cm^3$ of metal nitrides (see Table 2.2). The quantity of nitrogen desorption is almost comparable to the 1st cycle. In addition, this value fairly agreed with the amount of ammonia product determined by monitoring the pH value of the H_2SO_4 solution trap before and after hydrogenation as listed in Table 2.3. This result implies that a novel reaction process for nitrogenation using nitrogen storable intermetallic compounds should be developed. Aika et al. [45, 46] have reported that rare earth oxide-promoted Ru metal catalysts effectively produce ammonia at atmospheric pressure with a rate of 300-800 $\mu mol\ g^{-1}\ h^{-1}$. Meanwhile, the amount of ammonia product over the Ru/Al_2O_3/a-$TiFe_2$ composite material per one nitrogenation-hydrogenation cycle was 324 $\mu mol\ g^{-1}$. This value is not small compared with the rare earth oxide-promoted Ru metal catalyst, because the surface area of the

$TiFe_2$ powder used here was only 0.24 m^2 g^{-1}, while that of the rare earth

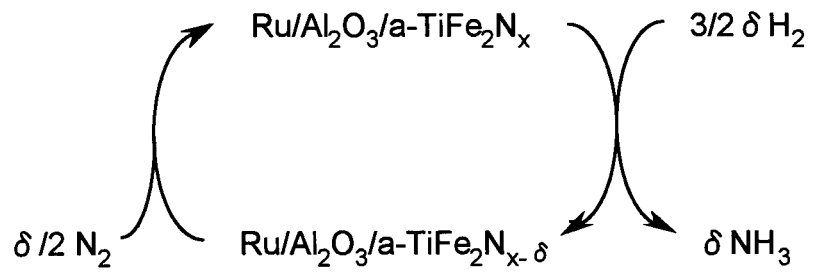

Fig. 2.8. A schematic model for a novel nitrogenation reaction using nitrogen storage material.

oxide-supported Ru metal catalyst was estimated to be 35 m^2 g^{-1} from the literature at least [46]. Figure 8 shows a schematic model for new nitrogenation reaction using the composite metal nitrides as proposed in this study.

2.4 Conclusions

The crystal Laves-phase compounds MFe_2 (M=Ti, Zr, Nb, and Mo) transform to the amorphous-like phase induced by the nitrogenation in the NH_3-H_2 mixed gas at 450 °C for 3 h, although such kinds of amorphization do not occur by the hydrogenation. This fact indicates that the nitrogen-induced amorphization easily takes place compared with the hydrogen-induced one owing to the difference in the atomic radius between nitrogen and hydrogen. A similar structural modification behavior is also observed on the σ-phase VFe compound with the layered structure.

The intermetallic compounds MFe_2 and VFe reversibly absorb and desorb large amounts of nitrogen in the amorphous-like metal nitride, when ammonia is used as nitrogen source. In the nitrogen desorption step, most of the nitrogen released from the metal nitrides reacts with hydrogen to produce ammonia owing to the high reactivity of atomic nitrogen liberated from the metal nitrides. Additionally, the amorphous-like MFe_2N_x show good stability against the nitrogen absorption-desorption cycle. The $Ru/Al_2O_3/a\text{-}TiFe_2N_{x-\delta}$ composite powder, which is once amorphized by the

nitrogenation in NH_3-H_2 and subsequently hydrogenated in H_2, can absorb nitrogen even using inert molecular nitrogen as the nitrogen source, and the resulting metal nitride releases nitrogen as ammonia by heating in H_2 at ambient pressure. The amount of ammonia product in one nitrogenation-hydrogenation cycle is about 324 μmol g^{-1}, which allows us to develop a novel process for nitrogenation reaction using the interstitial metal nitrides.

Chapter 3

Nitrogen Absorption and Desorption Characteristics over Rare earth-Iron Intermetallic Compounds

3.1 Introduction

In chapter 1, from the nitrogenation and hydrogenation characteristics of intermetallic compounds R_2Fe_{17} (R=Y, Ce and Sm), it has been found that significant amounts of nitrogen are absorbed by heating in the NH_3–H_2 mixed gas and the resulting metal nitrides reversibly desorbed the nitrogen as NH_3 by heating them in H_2 at 450 °C. Besides R_2Fe_{17}, other rare earth-iron intermetallic compounds with chemical formula of RFe_7 and RFe_2 have been studied by some workers [47-51]. RFe_7 and RFe_2, which possess the interstitial free spaces in crystal lattices to accommodate nitrogen, are expected to absorb and desorb nitrogen in a similar manner as the R_2Fe_{17} compounds. It is noted that the atomic arrangement for RFe_7 is intermediate between those of $CaCu_5$- and Th_2Zn_{17}-type structures and this structure is regarded as the iron deficient Th_2Zn_{17}-type structure, so that it is expected that the nitrogen more easily diffuses in the RFe_7 crystal lattices than that in R_2Fe_{17} ones.

In this chapter, rare earth-iron intermetallic compounds were prepared. The nitrogenation and hydrogenation were performed for these compounds in NH_3 or N_2 and H_2 in a temperature range of 250-450 °C to investigate the nitrogen absorption-desorption properties. Additionally, in order to promote the dissociation of molecular nitrogen as a nitriding gas, ruthenium metal catalyst (Ru/La_2O_3) was loaded on the surface of the $CeFe_7$ particles. The nitrogen storage and ammonia production properties using N_2 as the nitrogenation source were studied by cycling the nitrogenation and hydrogenation processes.

3.2 Experimental

The RFe_7 (R=Ce, Nd, Sm) and $CeFe_2$ compounds were prepared from appropriate amounts of rare earth metal shots or ingots (>99% in purity) and Fe wire (>99.9% in purity) by the conventional arc melting method in Ar atmosphere. The ingots of intermetallic compounds obtained were annealed in He at 800 °C for 48 h, and then crushed and pulverized into fine powders with diameters below 50 μm. For a part of the $CeFe_7$ powder, the Ru-La_2O_3 catalyst was loaded on the surface of $CeFe_7$ by the mechanical grinding method. La_2O_3 was heated in a flow of H_2 gas at 600 °C for 5 h to remove the moisture before use. La_2O_3 and $CeFe_7$ (molar ratio, La_2O_3:$CeFe_7$ = 1:5) were mixed in the N_2 gas atmosphere using a planetary-type ball mill. Ru was subsequently loaded on the surface of the La_2O_3–$CeFe_7$ composite powder by impregnation in a $Ru_3(CO)_{12}$-hexane solution via the decarbonylation by heating in H_2 at 573 K.

The intermetallic compounds prepared were identified on basis of powder X-ray diffraction patterns measured on a MAC Science M18XHF-SHA diffractometer using Cu Kα radiation equipped with a curved graphite monochlometer. The surface area values for the intermetallic compound powders were measured by a conventional BET method, together with those of Fe and Ce powders. The BET surface area values of all the samples studied in this study were almost similar to one another (0.16-0.24 $m^2\ g^{-1}$).

Every weighed powder (1 g) of RFe_7, R_2Fe_{17}, and RFe_2 was charged in each conventional fixed-bed quartz tube (12 mm *o.d.*), and the nitrogenation was made for them in the temperature range of 250-450 °C for 3 h in the respective streams of NH_3, NH_3-H_2, or N_2 gas with a flow rate of 30 ml/min. The hydrogenation was subsequently carried out for the respective nitrogenated samples at 450 °C for 3 h in the H_2 stream of the flow rate as that of NH_3 or N_2 for the nitrogenation. Nitrogen contents of nitrogenated and hydrogenated samples were measured by a nitrogen/oxygen analyzer (Horiba, EMGA 550) and the amount of the nitrogen regenerated from the metal nitride was calculated from the difference between their respective nitrogen contents. Nitrogen

species derived from the metal nitrides in the hydrogenation, that is, the nitrogen desorption step were collected in a liquid nitrogen trap and characterized on a mass spectrometer. The nitrogen regenerated as ammonia was quantified by monitoring the pH values of H_2SO_4 solution in the trap before and after passing the stripping gas from the metal nitride powder in the hydrogenation step.

The catalytic activities of ammonia decomposition over the RFe_7 and R_2Fe_{17} powders were measured by a gas chromatograph (Shimadzu GC-8A) in a temperature range of 200 °C-750 °C. The inlet gas was 5% NH_3 and He was used as a balance gas with a flow rate of 20 ml min^{-1}. The decomposition yield (conversion) from NH_3 to N_2 over the powdered samples was calculated by integrating their peak area ratio.

3.3 Results and discussion

The XRD patterns for the RFe_7 and RFe_2 powders prepared in this study were mainly indexed on the rhombohedral symmetry with space group of $R\bar{3}m$ and C15 Laves phase with space group of Fd3m, respectively. Figure 3.1 shows the XRD patterns for $CeFe_7$ heated in NH_3 at 400 °C for 1 h and in H_2 at 450 °C for 3 h, together with the as-obtained one. As shown in Fig. 3.1a, the diffraction patterns of the as-obtained $CeFe_7$ compounds fairly agreed with the crystal data reported by Ray [47]. There are seven formula units in the crystallographic primary cell, and the crystal structure of the RFe_7 phase prepared by the arc melting consists of the intermetallic atom arrangement between the $CaCu_5$- and Th_2Zn_{17}-type ones. This type of crystal structure is composed of one AB_5 layer alternating with two A_2B_{17} layers, *i. e.* $3AB_5 + 2A_2B_{17} = 7AB_7$ [47]. The XRD patterns for the RFe_7 prepared by arc melting are obviously distinct from the patterns reported elsewhere [48-50]. It seems that the structural arrangement of the resulting RFe_7 is greatly affected by the preparation methods, by the arc melting, self-flux crystal growth, rapid quenching and mechanical alloying. For the $CeFe_7$ sample prepared in this work, in

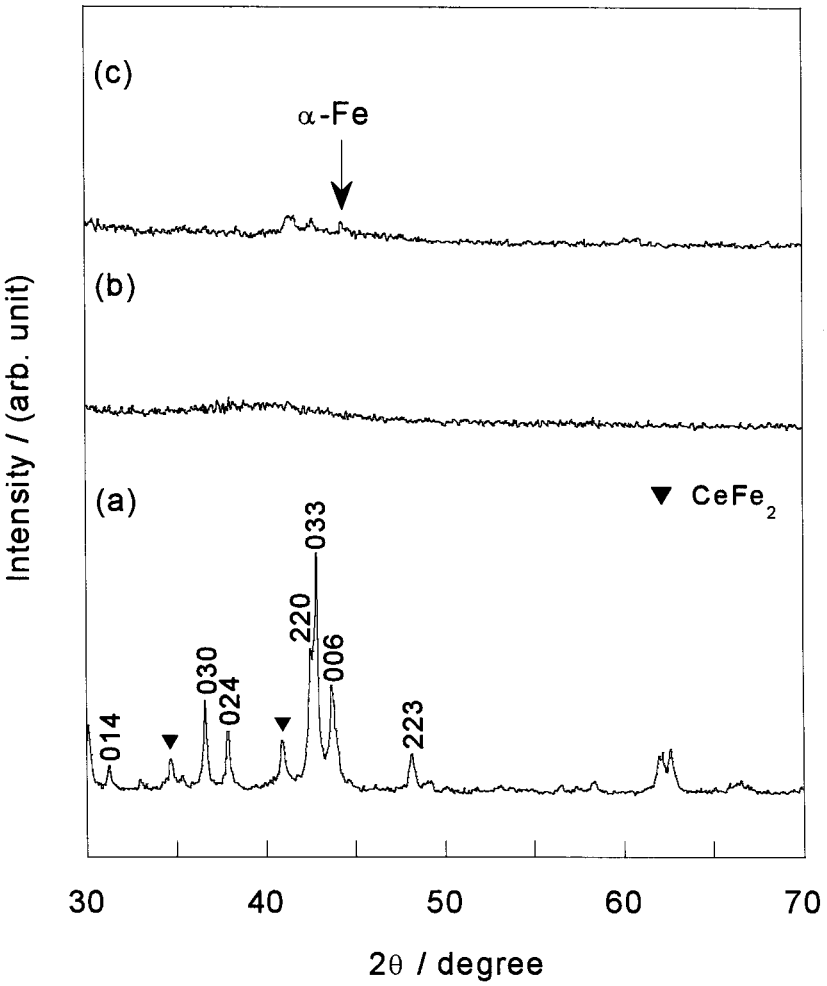

Fig. 3.1. XRD patterns of the $CeFe_7$ powders: a) untreated (as-obtained), b) nitrogenated in NH_3 at 400 °C for 1 h, and c) hydrogenated in H_2 at 450 °C for 3 h. Nitrogen contents x in the b) and c) samples are calculated to be 4.31 and 2.10 as the converted values per chemical formula unit of the starting material $CeFe_7$.

addition, weak peaks of $CeFe_2$ were also observed on the XRD patterns (see Fig. 3.1a). The phase diagram in the Ce-Fe binary system suggests that the $CeFe_2$ and $CeFe_7$ compounds are usually formed peritectically by the conventional arc melting method [51]. Figure 3.1b shows the diffraction pattern for RFe_7 after nitrogenation in NH_3 at 400 °C (nitrogen absorption). The diffraction peaks for the $CeFe_7$ powder disappeared by the nitrogenation, indicating that the crystalline $CeFe_7$ phase transformed to the amorphous one as seen in the Laves phase compounds such as $TiFe_2$. Similar amorphization was

observed on the nitrogenated $CeFe_2$ powder. After the hydrogenation (nitrogen desorption) in H_2 at 450 °C for 3 h for $CeFe_7N_x$, the weak diffraction peaks of α-Fe phase and $CeFe_7N_x$ were observed on the XRD pattern (see Fig. 3.1c). $CeFe_7N_x$ is the metastable compound, so that a part of $CeFe_7N_x$ decomposed and generated the precipitation of α-Fe. Amorphous $CeFe_7N_x$ was recrystallized by the desorption of nitrogen, although the peak intensity was considerably weak, suggesting that the crystallinity of $CeFe_7N_x$ was very low.

Figure 3.2 shows a typical mass spectrum for the nitrogen species regenerated from the $CeFe_7N_x$ powder by heating in H_2 at 450 °C for 3 h. The mass signals were appeared at the m/z values of 2, 15, 16 and 17, which were assigned to H_2^+, NH^+, NH_2^+ and NH_3^+ ions, respectively. Since H_2^+ is mainly originated from the H_2 stripping gas used here, NH_3 is responsible for the fraction ion species of NH^+, NH_2^+ and NH_3^+. It is concluded that the nitrogen absorbed in the RFe_7 crystal lattices is regenerated as NH_3 by reacting with H_2

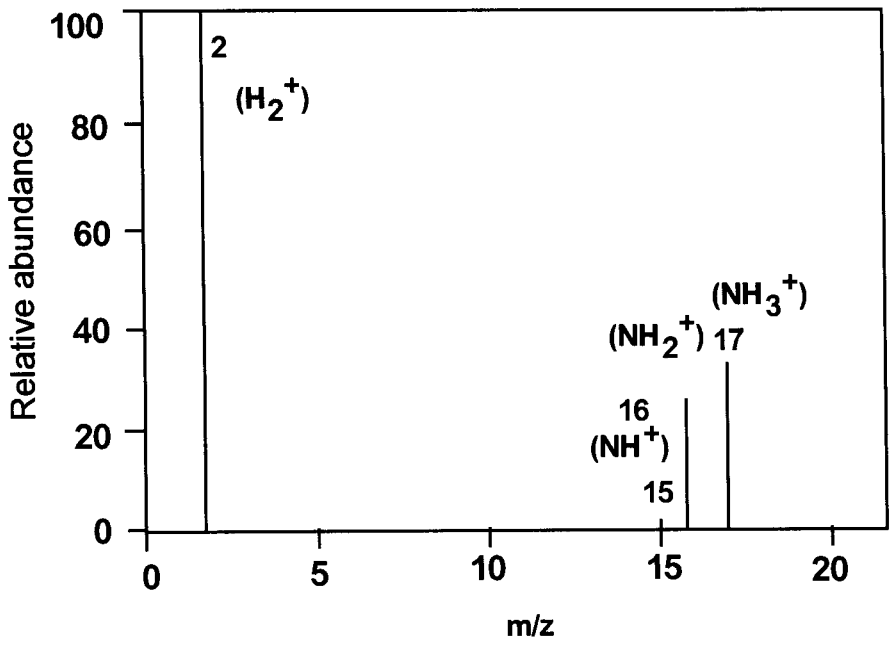

Fig. 3.2. Typical mass spectrum for the nitrogen species eluted from the amorphous (Ce, Fe)N_x with a converted composition of $CeFe_7N_{3.1}$ with H_2.

because any signals for the ion species derived from N_2 are not observed. The amounts of ammonia product determined by monitoring the pH values of H_2SO_4 solution trap before and after passing the H_2 gas were in good accordance with the quantities of the desorbed nitrogen as directly determined for the nitrogenated and hydrogenated metal nitrides by nitrogen analysis. It can be seen from these results that the atomic nitrogen released from the nitrogenated $CeFe_7$ powder is converted to ammonia at about 100% of yield.

The nitrogen absorption and desorption characteristics of the $CeFe_2$, $CeFe_7$, and Ce_2Fe_{17} powders observed on the nitrogenation in NH_3–H_2 at 450 °C for 3 h and on the hydrogenation in H_2 at 450 °C for 3 h are summarized in Table 3.1. The properties of nitrogen absorption and desorption on the Th_2Zn_{17} type compounds were superior to the C15 laves phase type one. In Th_2Zn_{17} type compounds, RFe_7 type compound, which is iron deficient Th_2Zn_{17} type structure, can absorb and desorb larger amounts of nitrogen compared with R_2Fe_{17} type compound. The smaller ammonia regeneration over the $CeFe_2$ powder was presumably due to the less activity of ammonia dissociation over the surface of $CeFe_2$, since the same type C15 Laves phase compound, $ZrFe_2$, can absorb a large amount of nitrogen (see Table 2.1 in Chapter 2).

The nitrogenation in NH_3 proceeds *via* the dissociation of ammonia over the surface

Table 3.1. Nitrogen absorption and desorption characteristics for $CeFe_2$, $CeFe_7$, and Ce_2Fe_{17}

Metal	Nitrogen content (x)		Regenerated ammonia
nitride (M.N.)	Nitrogenated	Hydrogenated	(mmol cm^{-3} of M.N.)[b]
$CeFe_2N_x$	1.2	0.9	11.33
$CeFe_7N_x$	3.3	0.6	28.30
$Ce_2Fe_{17}N_x$	6.6	3.7	16.96

a) Nitrogen contents x of the samples are represented as the values per chemical formula unit.

b) The amount of ammonia regenerated is calculated by assuming that the nitrogen released from 1 cm^3 of metal nitride is converted to ammonia.

of the intermetallic compounds as following equilibrium.

$$NH_3 \Leftrightarrow 3/2H_2 + N \qquad \Delta G^0 = 98450 - 42.3T \quad (J) \qquad (3.1)$$

From the Eq. 3.1, the activity of atomic nitrogen is represented as following equation.

$$a_N = \frac{P_{NH_3}}{P_{H_2}^{3/2}} \exp(-\frac{\Delta G^0}{RT}) \qquad (3.2)$$

From equation 3.2, it is obvious that the nitrogenation in sole NH_3 is more preferable than that in a NH_3-H_2 mixed gas with the consideration of the H_2 partial pressure, although H_2 in the nitrogenation by NH_3-H_2 mixed gas plays a role of easy nitrogen diffusion in the lattice due that the previous insertion of hydrogen into the crystal lattice accompanies the lattice expansion. So the nitrogen absorption and desorption characteristics of the R_2Fe_{17} and RFe_7 powders by the nitrogenation in NH_3 at 450 °C for 3 h and hydrogenation in H_2 at 450 °C for 3 h were performed (Table 3.2). Change of nitrogenation atmosphere from NH_3-H_2 to NH_3 allows absorbing large amounts of nitrogen over both R_2Fe_{17} and RFe_7. This result suggests that nitrogenation by sole NH_3 is more suitable than that by NH_3-H_2 mixture. The nitrogen absorption and desorption properties over the RFe_7 type

Table 3.2. Nitrogen absorption and desorption characteristics for the R_2Fe_{17} and RFe_7

Metal	Nitrogen content (x)		Regenerated ammonia
nitride (M.N.)	Nitrogenated	Hydrogenated	(mmol cm^{-3} of M.N.)[a)]
$Ce_2Fe_{17}N_x$	8.86	4.28	31.82
$Nd_2Fe_{17}N_x$	8.06	3.56	31.25
$Sm_2Fe_{17}N_x$	9.01	4.43	31.82
$CeFe_7N_x$	4.32	2.10	36.16
$NdFe_7N_x$	4.08	1.81	33.21
$SmFe_7N_x$	4.15	1.85	33.92

a) The amount of ammonia regenerated is calculated by assuming that the nitrogen released from 1 cm^3 of metal nitride is converted to ammonia.

compounds surpass the R_2Fe_{17} type ones in also this nitrogenation condition. Fe (6c) site is partially occupied (occ=2/3) in the crystallographic cell for $CeFe_7$, whereas Fe (6c) site is fully occupied (occ=1) for Ce_2Fe_{17}. It is concluded that the difference of nitrogen absorption and desorption properties between $CeFe_7$ and Ce_2Fe_{17} are contributed to the difference of crystal structure among them. If the nitrogen absorption and desorption behavior obeys a parabolic time law and reaction between metal and nitrogen is sufficient fast, the nitrogen diffusion in the bulk represented as Eq. 2.1 (see Chapter 2). It is necessary that the change of nitrogen concentration is proportional to the square root of the reaction time from equation 2.1. Figure 3.3 shows the time dependence of the amount of nitrogen desorption for $CeFe_7N_{3.0}$ and $Ce_2Fe_{17}N_{7.54}$ in H_2 flowing at 300 °C. As the good linearity was observed between the amount of nitrogen desorption and square root of the reaction time, the activation energies for nitrogen diffusion were evaluated from the nitrogen desorption rates for the nitrogenated specimen $CeFe_7N_{3.0}$

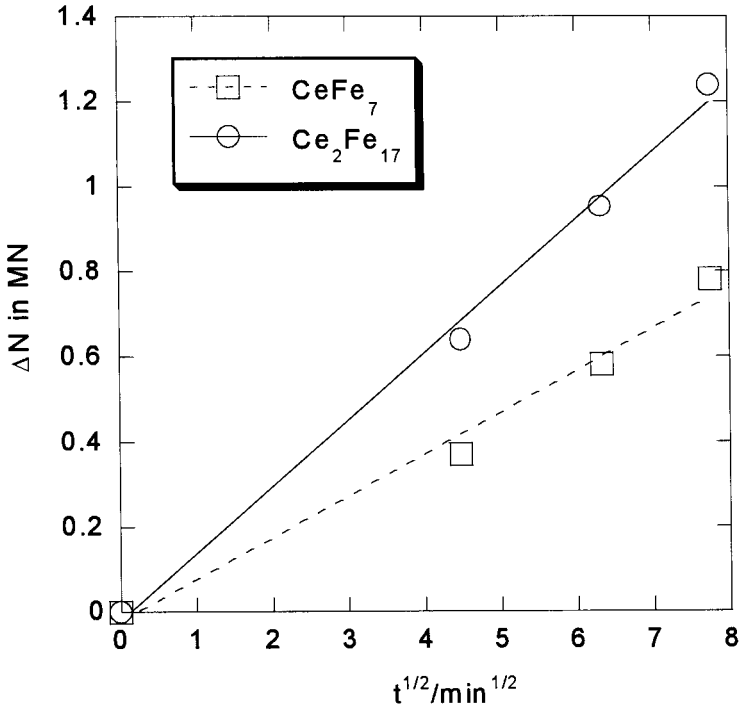

Fig. 3.3. Amount of Nitrogen desorption vs. the square root of the reaction time over $CeFe_7N_x$ and $Ce_2Fe_{17}N_x$.

and $Ce_2Fe_{17}N_{7.54}$ in the temperature range 250-350 °C (see Fig. 3.4). The activation energies of nitrogen diffusion are 69.3 and 101.6 kJ/ mol for $CeFe_7$ and Ce_2Fe_{17}, respectively. The crystal structure of $CeFe_7$ is regarded as a kind of iron deficient Th_2Zn_{17}-type structure. Therefore, the nitrogen atoms diffuse more easily in $CeFe_7$ than that in Ce_2Fe_{17} through iron-deficient sites of the former ones. One of the reasons for the superior property of nitrogen absorption and desorption observed on $CeFe_7$ is responsible for the ease of nitrogen diffusion in the bulk compared with Ce_2Fe_{17}.

To compare the nitrogen storage properties for $NdFe_7$ and Fe, the nitrogen absorption and desorption characteristics of the $NdFe_7$ and Fe powders by the nitrogenation in NH_3 at 300-450 °C for 1-3 h and hydrogenation in H_2 at 450 °C for 3 h were conducted (Table 3.3). Even for the nitrogenation at 300 °C, $NdFe_7$ absorbed nitrogen to form the corresponding metal nitride $NdFe_7N_{1.88}$. The nitrogen content decreased down to $NdFe_7N_{0.89}$ after the subsequent hydrogenation made by the heat

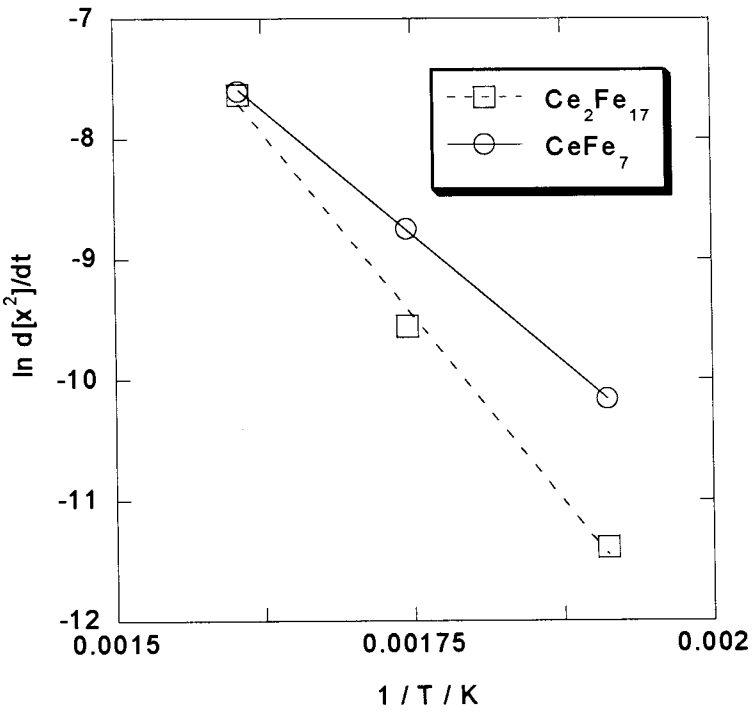

Fig. 3.4. Arrhenius plot s of the nitrogen desorption rate of $CeFe_7$ and Ce_2Fe_{17}.

treatment in H_2 at 450 °C. The Fe metal powder, however, was hardly nitrogenated under the same condition. This fact indicates that $NdFe_7$ is more effectively nitrogenated than Fe. By calculating based on the difference of nitrogen content (Δx=0.99) between $NdFe_7N_{1.88}$ (after nitrogenation) and $NdFe_7N_{0.89}$ (after hydrogenation), the quantity of the nitrogen desorbed from 1 cm^3 of the metal nitride (ρ=*ca.*7.83 g cm^{-3}) was converted to 14.46 mmol of NH_3, because the atomic nitrogen stored in the crystal lattice was released as NH_3 at about 100% of yield in the desorption step (see Fig. 3.2).

Table 3.3. Nitrogen absorption and desorption characteristics for the $NdFe_7$ and Fe

Metal nitride (M.N.)	Cycle number	Nitrogen content (x)		Regenerated ammonia (mmol cm^{-3} of M.N.)[b]
		Nitrogenated	Hydrogenated	
(A) Nitrogenation in NH_3 at 300 ℃for 3 h				
$NdFe_7N_x$	1	1.88	0.89	14.46
FeN_x	1	0	0	0
(B) Nitrogenation in NH_3 at 450 ℃for 1 h				
$NdFe_7N_x$[a]	1	3.90	1.93	28.83
FeN_x	1	0.18	0.001	25.26
(C) Nitrogenation in NH_3 at 450 ℃for 3 h				
$NdFe_7N_x$[a]	1	4.08	1.81	33.21
	10	3.43	0.83	38.03
FeN_x	1	0.27	0.001	37.67

a) Nitrogen contents x of the RFe_7N_x samples are represented as the values per chemical formula unit.
b) The amount of ammonia regenerated is calculated by assuming that the nitrogen released from 1 cm^3 of metal nitride is converted to ammonia.

The nitrogenation at 450 °C allowed the RFe_7 crystal lattices to absorb the much more amounts of nitrogen than that at 300 °C, owing to the enhanced nitrogen diffusion rate. As described above, however, the crystal lattices of RFe_7 were amorphized and $NdFe_7$ partly decomposed to precipitate α-Fe during the nitrogen absorption and desorption for them. Thus, such large amounts of nitrogen should be understood to be

stored in the composite materials, Fe/a-(Nd, Fe)N_x. Amounts of the ammonia regenerated from the Fe/a-(Nd, Fe)N_x composite powders were evaluated to be 33.21 mmol per 1 cm^3 of the metal nitrides on the basis of the nitrogen analysis data for the nitrogenated and hydrogenated $NdFe_7$ one. It is noted that the amounts of the nitrogen regenerated from 1 cm^3 of Fe/a-(Nd, Fe)N_x are 2.8 times larger than those of the conventional high-pressure nitrogen containers charged at 15 MPa (6.12 mmol of N_2 gas per 1 cm^3 of their containers' volume). Nd metal used as the starting materials were inactive for the dissociation of NH_3 at 450 °C to yield no metal nitride, and only a trace of NdN was observed during the nitrogenation at 700 °C. The Fe powder (particle size about 50 μm) also hardly reacts with NH_3 at 300 °C, whereas the RFe_7 intermetallic compounds can incorporate large amounts of nitrogen into their lattices. By raising the reaction temperature, however, a considerable amount of nitrogen was absorbed in the Fe crystal lattice. Consequently, the regenerated ammonia amounted to 37.6 mmol per 1 cm^3 of FeN_x, although the formation of iron nitrides was required the higher reaction temperature compared with that of RFe_7. The XRD pattern of nitrogenated Fe powder was mixed with those of Fe_3N and Fe_4N. The amount of the ammonia regenerated for the Fe powder was comparable to that for the RFe_7 one in 10th cycle. In the case of nitrogenation for 1 h, the resulting quantity of ammonia for $NdFe_7$ is superior to that for Fe. The RFe_7 intermetallic compounds can absorb nitrogen faster than Fe under the more moderate reaction conditions.

The nitrogen storage capacity of $NdFe_7$ compounds increased with repeating the nitrogen absorption-desorption cycle. The amount of the ammonia regenerated from the Fe/a-(R, Fe)N_x composite powder in the 10th cycle (38.03 mmol) was higher than that in the first cycle (33.21 mmol). The XRD pattern of composite material after 10th nitrogenation was mixed with those of Fe_3N and a-(Nd, Fe)N_y. This means that these kinds of composite materials, Fe_3N/a-(R, Fe)N_y, give such excellent nitrogen absorption and desorption characteristics. It is concluded that the FeN_x/a-(R, Fe)N_y composite material is also highly active for the dissociation of NH_3. In the study of ammonia

synthesis over rare earth intermetallic compounds by Takeshita *et al.* [28], it has been reported that these intermetallic compounds decompose to α-Fe and RN during the reaction of N_2-H_2 mixed gas under a pressure of 7 MPa and the resulting α-Fe/RN composite materials are highly active for the production of ammonia.

Figure 3.5 shows scanning electron microscope photographs of the as obtained, 1st, and 10th nitrogenated $NdFe_7$ powders. As seen in Fig. 3.5a, it was found that many cracks occurred on the surface of the $NdFe_7$ particles because of the lattice expansion by absorbing large size of nitrogen atom interstitially. After the 10th nitrogenation cycle (see Fig. 3.5b), the particle size became smaller than the 1st one due to the lattice strain by nitrogen absorption and the phase separation took place between FeN_x and a-(Nd, Fe)N_y much more. The tendency that the amount of the ammonia regenerated from the metal nitride increases in 10th cycle is ascribed to the enlargement of the surface area since the crack formation becomes so frequent on the surface of the RFe_7 particles *via* the expansion and shrinkage of the lattices induced by repeating the nitrogen

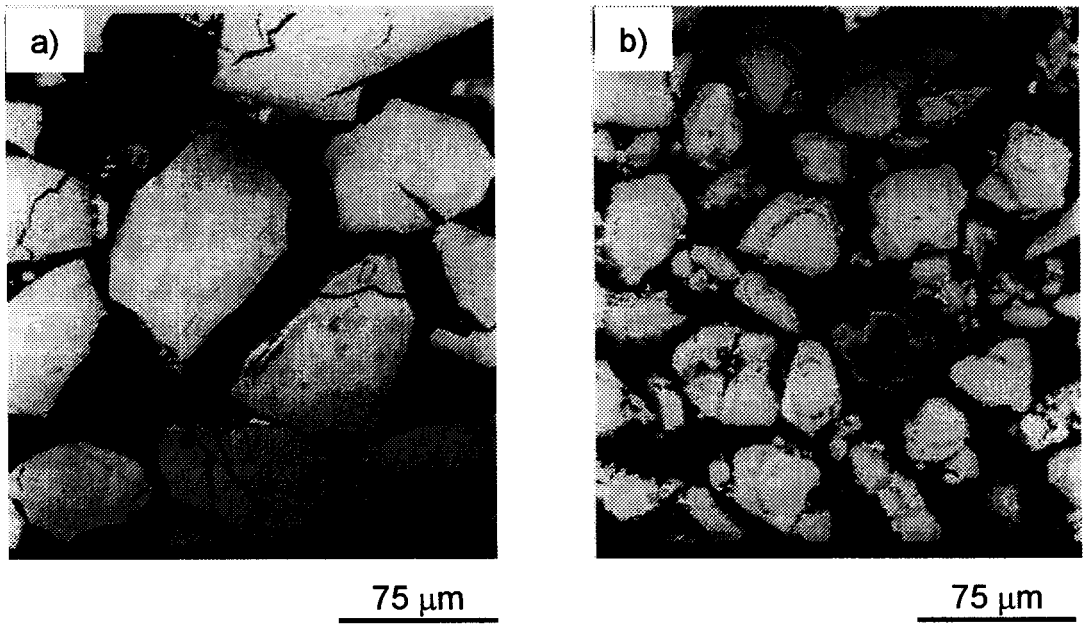

Fig. 3.5. SEM photographs of $NdFe_7N_x$ and the derived composite materials: a) 1st and b) 10th nitrogenated in NH_3.

absorption-desorption cycle and the high activity for the dissociation of NH_3 molecules over the Fe_3N/a-(Nd, Fe)N_y composite materials.

Figure 3.6 shows the decomposition characteristics of ammonia over the $NdFe_7$ and Fe powders. The temperature to start the dissociation of ammonia over the $NdFe_7$ powder was lower than that over the Fe powder. This result indicates that the activity for the dissociation of ammonia over the $NdFe_7$ powder is higher than that of the Fe powder. The ammonia dissociation characteristics over the $NdFe_7$ and Fe powders fairly agreed with their nitrogen absorption properties as summarized in Table 3.3. Therefore, the nitrogenation over the RFe_7 compounds is expected to take place faster than Fe, so that ammonia is reproduced by cycling the nitrogenation and hydrogenation processes alternately in nitrogenation even at 300 °C.

As mentioned above, the RFe_7 intermetallic compounds can reversibly absorb and desorb significant amounts of nitrogen, and the nitrogen incorporated into the crystal lattices is easily converted to ammonia in the nitrogen desorption (hydrogenation) step.

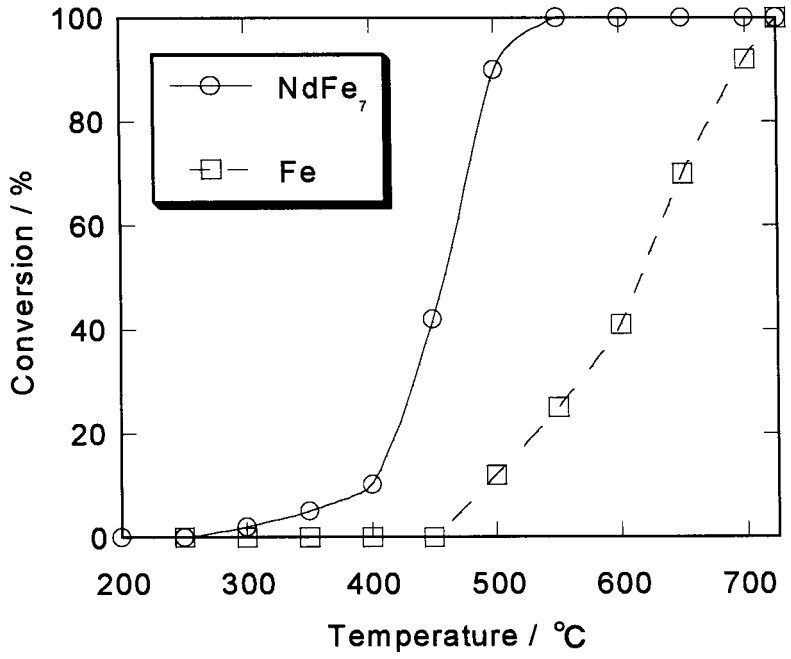

Fig. 3.6. Decomposition characteristics of ammonia over the $CeFe_7$ and Fe powders.

However, this nitrogen absorption-desorption system is less important in the viewpoint of the chemical engineering for use of ammonia as nitrogenation source. If molecular nitrogen is used as such nitrogen source, it is possible to develop novel reaction process using atomic nitrogen by which molecular nitrogen can be eventually converted to ammonia *via* the nitrogenation-hydrogenation cycle for the intermetallic compounds. For the catalytic approaches, the ammonia synthesis has been already tried over the rare earth-transition metal intermetallic compounds (*e.g.* $CeRu_2$, $HoFe_3$, and $PrCo_5$) by Takeshita and coworkers [28]. After conducting the reaction, the crystal structure of $HoFe_3$ completely decomposed to HoN and α-Fe. This result suggests that HoN hardly releases nitrogen owing to its great stability of ionic bonding-type nitride and the ammonia formation by the direct reaction between N_2 and H_2 gas (under a high pressure condition of about 7MPa) mainly takes place on the surface of transition metal promoted by electron transferring from rare earth nitrides such as HoN. In this study, the nitrogenation and hydrogenation processes are performed alternately in the individual N_2 and H_2 streams, and consequently, the atomic nitrogen desorbed from the metal nitride is converted to ammonia in the desorption step under atmospheric pressure.

The nitrogenation for $CeFe_7$ was conducted in N_2 instead of NH_3 by heating at 673 K for 3 h. The nitrogen content per chemical formula was 0.70. The subsequent nitrogen desorption was carried out in H_2 at 723 K for 3 h to desorb nitrogen down to $CeFe_7N_{0.66}$. The amount of ammonia product per unit volume was only 0.58 mmol that sharply decreased compared with the case of nitrogenation in NH_3. The respective binding energy of N-H and N≡N are 431 and 941 kJ mol^{-1}. The dissociation of strong triple bonding of N_2 is assumed to be rate determining step for nitrogen absorption reaction. It is well known that ammonia is more favorable as the nitrogen source than molecular nitrogen in the points of thermodynamics [52]. To accelerate the dissociation ability for molecular nitrogen, the composite material between the Ru/La_2O_3 catalyst (15 wt. %) and the $CeFe_7$ intermetallic compound (85 wt. %) was prepared by the mechanical

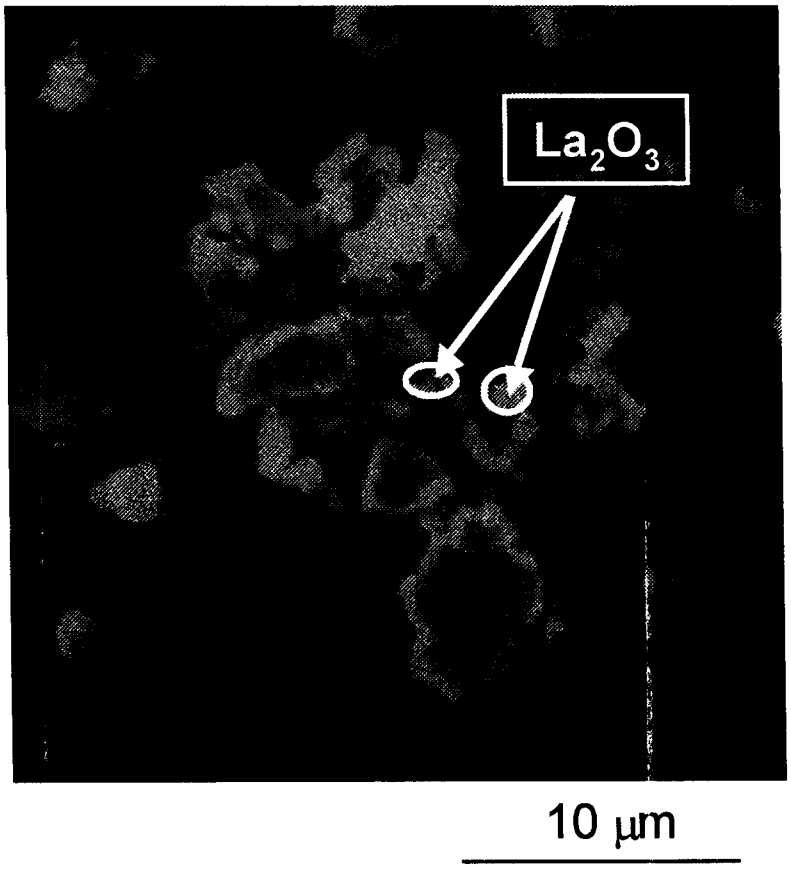

Fig. 3.7. Scanning electron microscope photograph of the Ru/La_2O_3-$CeFe_7$ composite powder.

grinding method, of which the Ru/La_2O_3 catalyst plays a role of promoting the dissociation of molecular nitrogen reported by Aika et al [46]. From the scanning microscope measurement with an EPMA analysis, it was confirmed that the La_2O_3 was loaded on the surface of $CeFe_7$ (see Fig. 3.7).

For the Ru-La_2O_3/$CeFe_7$ composite powder, the nitrogenation was performed at 673K in N_2 for 3 h. The amount of nitrogen absorption per chemical formula increased to be 1.56. After the subsequent nitrogen desorption by heating at 473K in H_2 for 3 h, the nitrogen content per chemical formula unit decreased to 1.38, resulting that the amount of ammonia product per unit volume was up to 2.91 mmol. At 5th cycle for nitrogen absorption and desorption over Ru-La_2O_3/$CeFe_7$, the nitrogen content per

chemical formula unit after nitrogenation was 1.65, whereas 1.43 after denitrogenation. The amount of ammonia product per unit volume was consequently 3.55 mmol (Table 3.4). Ru-La_2O_3/$CeFe_7$ showed a good durability for nitrogen absorption-desorption cycle. The resulting amount of ammonia product per 1 g of $CeFe_7$ at 5th cycle is 452 μmol. From these results, the Ru-La_2O_3/$CeFe_7$ composite material can store highly reactive atomic one in the crystal lattice with a capacity of 40 times volume of nitrogen per its unit volume. Since the highly reactive monoatomic nitrogen easily reacts with

Table 3.4 Nitrogen absorption and desorption characteristics for $CeFe_7$ and Ru-La_2O_3/$CeFe_7$

Metal nitride	Cycle number	Nitrogen content (x)[a]		Regenerated ammonia ($mmol/cm^3$)
		After nitrogenation	After hydrogenation	
$CeFe_7N_x$	1	1.31	1.21	1.6
Ru-La_2O_3 /$CeFe_7N_x$	1	1.56	1.38	2.91
	5	1.65	1.43	3.55

a) Nitrogen contents are represented as the values per chemical formula unit.

hydrogen to generate ammonia at about 100 % of yield, it is concluded that the above nitrogen absorption-desorption reactions is regarded as a new process of ammonia synthesis using the formation of interstitial type metal nitrides.

3.4 Conclusions

Rare earth-iron intermetallic compounds RFe_7 (R=Ce, Nd and Sm) reversibly absorb and desorb large amounts of nitrogen by cycling the respective nitrogenation and hydrogenation processes made in NH_3 and H_2 at 300-450 °C. The amounts of the nitrogen regenerated per unit volume of these compounds through the nitrogen absorption and desorption is larger than that of the conventional high pressure nitrogen cylinder charged

at 15 MPa. The nitrogen storage capacity of the RFe_7 compounds are superior to that of the R_2Fe_{17} ones since the crystal structure of RFe_7 is the iron deficient Th_2Zn_{17}-type one which is favorable for the nitrogen diffusion in the bulk. Additionally, the atomic nitrogen stored as the metal nitrides is regenerated as ammonia in the nitrogen desorption step in H_2 at about 100% of yield. The amount of the regenerated ammonia is increased with repeating the nitrogen absorption-desorption cycle of RFe_7 compounds and the formation of FeN_x/a-(R, Fe)N_y composite materials is responsible for the increase of nitrogen regeneration. Futhermore, RFe_7 can absorb nitrogen by the nitrogenation in N_2 at 400 °C even though molecular nitrogen is generally too hard to produce such metal nitrides because of the huge bonding energy. The resulting nitrides RFe_7N_x release the nitrogen as ammonia by heating in H_2. The Ru/La_2O_3-$CeFe_7$ composite powder was more easily nitrogenated by N_2 in order to promote the ability for dissociation of molecular nitrogen by Ru/La_2O_3 catalyst, resulting that the larger amounts of ammonia generation was than $CeFe_7$. Ru/La_2O_3-$CeFe_7$ can generate larger amount of ammonia compared with Ru-Al_2O_3/a-$TiFe_2$ even at lower temperature of nitrogenation in N_2.

Summary

Chapter 1.

The intermetallic compounds R_2Fe_{17} (R=Y, Ce, and Sm) formed the corresponding interstitial type metal nitrides by heating in a mixed gas of NH_3-H_2 at 350-450 °C. The nitrogen stored as the metal nitrides was reversibly desorbed as NH_3 at about 100% of yield by the following heating in H_2 at 450 °C. The amount of the nitrogen released per unit volume of these intermetallic compounds is larger than that of a conventional nitrogen container charged at 15MPa. The nitrogen storage capacity of $Sm_2Fe_{17}N_x$ increased by repeating the nitrogenation-hydrogenation cycles owing to the formation of FeN_x/a-(R, Fe)N_y composites with large surface areas derived from the starting intermetallic compound through nitrogenation and hydrogenation. Additionally, the nitrogen storage property of Sm_2Fe_{17} powder was effectively improved by surface modification with Ru metal loading.

Chapter 2.

Nitrogen absorption and desorption characteristics were conducted for the intermetallic compounds such as MFe_2 (M=Ti, Zr, Nb, and Mo) or M'Fe (M'=Ti and V) Among them, a series of the Laves-phase MFe_2 and σ-phase VFe compounds absorbed large amounts of nitrogen into the crystal lattices to transform to the amorphous-like metal nitrides, of which the randomized structures were induced by the insertion of large atomic size of nitrogen into the crystal lattices. These metal nitrides reversibly released the nitrogen by the following hydrogenation, and the amorphous-like structures were maintained after that. Furthermore, once such amorphous-like modification of $TiFe_2$ (a-$TiFe_2$) induced by the nitrogenation in the NH_3-H_2 mixed gas could absorb nitrogen even by the nitrogenation in N_2 gas with co-loaded with the ruthenium metal and aluminum oxide on the surface of $TiFe_2$. The nitrogen stored was also released as

ammonia in the subsequent hydrogenation under atmospheric pressure.

Chapter 3.

Reversible nitrogen absorption and desorption were observed on the rare earth-iron intermetallic compounds RFe_2 and RFe_7. In particular, the intermetallic compounds RFe_7 with the modified Th_2Zn_{17}-type structure absorbed large amounts of nitrogen into their crystal lattices. The nitrogen absorption and desorption properties over Th_2Zn_{17}-type RFe_7 were superior to those over Th_2Zn_{17}-type R_2Fe_{17} due to the ease of nitrogen diffusion in the bulk, since Fe (6c) site is partially occupied (occ=2/3) in the crystallographic cell for RFe_7, whereas Fe (6c) site is fully occupied (occ=1) for R_2Fe_{17}. Furthermore, $CeFe_7$ could absorb nitrogen even by nitrogenation in N_2 at 400 °C. The resulting metal nitride desorbed nitrogen as ammonia by subsequent. Ru-La_2O_3/$CeFe_7$ composite powder, which was active for dissociation for molecular nitrogen by loading Ru-La_2O_3 catalyst, can product more larger amount of ammonia than Ru-Al_2O_3/a-$TiFe_2$ even at lower nitrogenation temperature *via* the nitrogenation-hydrogenation cycle.

References

[1] K. H. J. Buschow, *Hydrogen Absorption in Intermetallic Compounds* in *Handbook on the Physics and Chemistry of Rare Earths*; ed. by K. A. Gschneidner Jr., L. Eyring, Elsevier: New York, 1984, Vol. 6, pp.1- 111.

[2] K. Soga, H. Imamura, and S. Ikeda, *J. Phys. Chem.*, **81**, 1762 (1977).

[3] J. R. Jhounson, Z. Gavra, and J. J. Reilly, *Z. Phys. Chem.*, **183**, 391 (1994).

[4] G. D. Sandrock and P. D. Goodell, *J. Less-common Met.*, 104, 159 (1984).

[5] S. Suda, K. Iwata, Y-M. Sun, Y. Komazaki, and F-J. Liu, *J. Alloys and Compd.*, **253,** 668 (1997).

[6] H-Y. Zhu, *J. Alloys and Compd.*, **240**, L1 (1996).

[7] M. Itoh, K. Machida, and G. Adachi, *Chem. Lett.*, 1056 (2000).

[8] H. Imai, T. Tagawa, and M. Kuranishi, *Mat. Res. Bull.*, **20**, 511 (1985).

[9] J. R. Johunson, Z. Gavra, P. Chyou, and J. J. Reilly, *J. Catal.*, **137**, 102 (1992).

[10] J. P. Collins and J. D. Way, *J. Membrane Sci.*, **96**, 259 (1994).

[11] J. P. Collins, J. D. Way, and N. Kraisuwansarn, *J. Membrane Sci.*, 77, 265 (1993).

[12] T. Iriyama, *Ph. D. Thesis. Zhejiang University*, (1990).

[13] T. Iriyama, K. Kobayashi and H. Imai, *European Patent Appl., Pub. num.*, 0-369-097 A1 (1989).

[14] J. M. D.Coey and H. Sun, *J. Magn. Magn. Mater.*, **87**, L251 (1990).

[15] R. Arlot, H. Izumi, K. Machida, D. Fruchart, and G. Adachi, *J. Magn. Magn. Mater.*, **172**, 119 (1997).

[16] H. Izumi, K. Machida, A. Shiomi, M. Iguchi, and G. Adachi, *Jpn. J. Appl. Phys.*, **35**, L894 (1996).

[17] K. Noguchi, M. Nishimura, K. Machida, and G. Adachi, *Chem. Lett.*, 555 (1999).

[18] K. Noguchi, M. Nishimura, K. Machida, and G. Adachi, *Chem. Lett.*, 793 (1999).

[19] K. Noguchi, M. Nishimura, K. Machida, and G. Adachi, *Chem. Mater.*, **11**, 2527 (1999).

[20] K. Noguchi, K. Machida, K. Yamamoto, M. Nishimura, and G. Adachi, *Appl. Phys. Lett.*, **75**, 1601 (1999).

[21] K. Machida, K. Noguchi, M. Nishimura, and G. Adachi, *J. Appl. Phys.*, **87**, 5317 (2000).

[22] Y. Otani, D. P. F. Hurley, H. Sun and J. M. D. Coey, *J. Appl. Phys.*, **69**, 5584 (1990).

[23] O. Isnard, S. Miraglia, J. L. Soubeyroux, D. Fruchart, J. Deportes and K. H. J. Buschow, *J. Phys.: Condens. Matter.*, **5**, 5481 (1993).

[24] R. M. Ibberson, O. Moze, T. H. Jacobs and K. H. J. Buschow, *J. Phys.: Condens. Matter.*, **3**, 1219 (1991).

[25] A. Ozaki, *Acc. Chem. Res.*, **14**, 16 (1981).

[26] K. Niwa and T. Yokokawa, *Kinzokuneturikigaku*, (1970).

[27] "Binary Alloy Phase Diagrams," ed. by T. B. Massalski, J. L. Murray, L. H. Bennett and H. Baker, Amer. Soc. Met., Metals Park, 1986, Vol. 1, pp. 1079-1083.

[28] T. Takeshita, W. E. Wallence, and R. S. Graig, *J. Catal.*, **44**, 236 (1976).

[29] J. J. Reilly and R. H. Wiswall. Jr., *Inorg. Chem.*, **13**, 218 (1974).

[30] T. Yamashita, T. Gamo, Y. Moriwaki, and M. Fukuda, *Nippon Kinzoku gakkaishi*, **41**, 148 (1977).

[31] Y. Kadowaki, K. Aika, *J.Catal.*, **161**, 178 (1996).

[32] C. C. Nagel, J. C. Bricker, D. G. Alway, and S. G. Shore, *J. Organomet. Chem.*, **219**, C9 (1981).

[33] V. Koeninger, H. H. Uchida, and H. Uchida, *J. Alloys Comp.*, **222**, 117 (1995).

[34] V. Paul-Boncour, A. Percheron-Guegan, M. Diaf, and J. C. Achard, *J. less-Common Met.*, **131**, 201 (1987).

[35] K. Aoki, X-G. Li, and T. Masumoto, *Acta. Metal. Mater.*, **40**, 1717 (1992).

[36] D. Fruchart, J. L. Soubeyroux, and R. Hempelmann, *J. Less-Common Met.*, **99**, 307 (1984).

[37] W. B. Pearson and W. J. Christian, *Acta. Cryst.*, **5**, 157 (1952).

[38] H. Uchida, S. Tachibana, T. Kawanabe, Y. Matsumura, V. Koeninger, H. H. Uchida, H. Kaneko, and T. Kurino, *J. Alloys and Comp.*, **222,** 107 (1995).

[39] J. M. D. Coey, R. Skomski, and S. Wirth, *IEEE Trans.*, **28**, 2332 (1992).

[40] E. Schwab and E. Wicke, *Z. Phys. Chem. N. F.*, **122**, 217 (1980).

[41] R. Kirch, R. Hempelmann, E. Schwab, and H. Zuchner, *Z. Phys. Chem. N. F.*, **126**,

109 (1981).

[42] P. Thompson, F. Reidinger, and J. J. Reilly, *J. Phys. F.*, **10**, L57 (1980).

[43] J. S. Kasper, B. F. Decker, and J. R. Belanger, *J. Appl. Phys.*, **22**, 361 (1951).

[44] W. Tucker, and C. W. Wallence Jr., *Acta. Cryst.*, **4**, 425 (1951).

[45] Y. Niwa and K. Aika, *J. Catal.*, **162**, 138 (1996).

[46] S. Murata, K. Aika, and T. Onishi, *Chem. Lett.*, 1067 (1990).

[47] A. E. Ray, *Acta. Cryst.*, **21**, 426 (1965).

[48] H. Samata, Y. Satoh, Y. Nagata, T. Uchida, M. Kai, and M. D. Lan, *Jpn. J. Appl. Phys.*, **36**, L476 (1997).

[49] M. K. Katter, J. Wecker, and L. Schultz, *J. Appl. Phys.*, **70**, 3188 (1991).

[50] A. Teresiak, M. Kubis, N. Mattern, M. Wolf, and K.–H. Müller, *J. Alloys Compds.*, **274**, 284 (1998).

[51] J. O. Jepson and P. Duwes, *Trans. Amer. Soc. Metals*, **47**, 543 (1955).

[52] M. Katsura, *J. Alloys Comp.*, **182**, 91 (1992).

Acknowledgments

The author would like to express his sincerest gratitude to Professor Gin-ya Adachi, Department of Applied Chemistry, Faculty of Engineering, Osaka University, for his continuous guidance throughout this work.

The author would like to express deeply thanks Professor Ken-ichi Machida, Collaborative Research Center for Advanced Science and Technology, Osaka University, for his helpful suggestions and fruitful discussions.

The author would like to thank Professor Toshikazu Hirao and Professor Yasuhiko Shirota, Department of Applied Chemistry, Faculty of Engineering, Osaka University, for their helpful comments and suggestions.

The author also wish to thank Associate Professor Nobuhito Imanaka, and Assistant Professor Toshiyuki Masui, Department of Applied Chemistry, Faculty of Engineering, Osaka University, for their heartfelt advice.

The author would like to express his sincerest thanks to Professor Hirotaro Mori, and Dr. Takao Sakata, Research Center for Ultra-High Voltage Electron Microscopy, Osaka University, for their help of transmission electron microscopy measurements and useful discussions.

The author desires to express his sincere thanks to Dr. Tetsuya Ozaki, National Research for Metals, for his valuable suggestions and heartfelt advices.

The author is grateful acknowledgments to Mr. Hiroharu Nakajima, Mr. Kazuhiro Hirose, and Ms. Misa Yamamoto for their pioneering research of this work. I would like to appreciate Mr. Masahiro Masuda, Mr. Ryo Hamada, Mr. Yu Hamaguchi, and Mr Kenji Noguchi, for their helpful assistance and support in the course of this work, and the author also wish to thank all the members of the research groups of Professor Gin-ya Adachi and Professor Ken-ich Machida, for their hearty supports, helpful advises, and

friendship.

Research Fellowships of the Japan Society for the promotion of Science for Young Scientists is greatly acknowledged.

Finally the author would like to express his special gratitude to his parents and sister for their encouragement and understanding on this work.